

1 Vertical profiles of volatile organic compounds and fine particles in 2 atmospheric air by using aerial drone with miniaturized samplers and 3 portable devices

4 Eka Dian Pusfitasari^{1,2}, Jose Ruiz-Jimenez^{1,2}, Aleksi Tiusanen¹, Markus Suuronen¹, Jesse Haataja³, Yusheng
5 Wu³, Juha Kangasluoma³, Krista Luoma^{3,4}, Tuukka Petäjä³, Matti Jussila^{1,2}, Kari Hartonen^{1,2*}, and Marja-
6 Liisa Riekkola^{1,2*}

7 ¹Department of Chemistry, P.O. Box 55, FI-00014 University of Helsinki, Finland

8 ²Institute for Atmospheric and Earth System Research, Chemistry, Faculty of science, P.O. Box 55, FI-
9 00014 University of Helsinki, Finland

10 ³Institute for Atmospheric and Earth System Research, Physics, Faculty of science, P.O. Box 64, FI-00014
11 University of Helsinki, Finland

12 ⁴Finnish Meteorological Institute, P.O. Box 503, FI-00101 Helsinki, Finland

13

14 *Corresponding authors: Dr. Kari Hartonen (kari.hartonen@helsinki.fi) and prof. Marja-Liisa Riekkola
15 (marja-liisa.riekkola@helsinki.fi)

16

17 **Abstract.** The increase of volatile organic compounds (VOCs) emissions released into the atmosphere is one
18 of the main threats to human health and climate. VOCs can adversely affect human life through their
19 contribution to air pollution directly and indirectly by reacting via several mechanisms in the air to form
20 secondary organic aerosols. In this study, aerial drone equipped with miniaturized air sampling systems
21 including up to four solid-phase microextraction (SPME) Arrows and four in-tube extraction (ITEX)
22 samplers for the collection of VOCs, along with portable devices for the real-time measurement of black
23 carbon (BC) and total particle numbers at high altitudes was exploited. In total, 135 air samples were collected
24 under optimal sampling conditions from October 4 to October 14, 2021 at the boreal forest SMEAR II Station,
25 Finland. A total of 48 different VOCs, including nitrogen-containing compounds, alcohols, aldehydes,
26 ketones, organic acids, and hydrocarbons, were detected at different altitudes from 50 to 400 m above ground
27 level with the concentrations up to 6898 ng m⁻³ in gas phase and 8613 ng m⁻³ in particle phase. Clear
28 differences in VOCs distribution were seen in samples collected from different altitudes, depending on the
29 VOC sources. It was also possible to collect aerosol particles by the filter accessory attached on the ITEX
30 sampling system, and five dicarboxylic acids were quantified with the concentrations of 0.43 to 10.9 µg m⁻³.
31 The BC and total particle number measurements provided similar diurnal patterns, indicating their
32 correlation. For spatial distribution, the BC concentrations were increased at higher altitudes being 2278 ng

33 m^{-3} at 100 m and 3909 ng m^{-3} at 400 m. The measurements onboard the drone provided insights into horizontal
34 and vertical variability in BC and aerosol number concentrations above the boreal forest.

35 **Keywords:** aerial drone; miniaturized air sampling systems; solid-phase microextraction Arrow; in-tube
36 extraction; volatile organic compounds; black carbon; total particle number.

37 1. Introduction

38 The global phenomenon of climate change has attracted a huge attention in the past decades. Atmospheric
39 aerosol particles can influence the climate system directly by scattering sunlight, transmission, and absorption
40 of radiation, and indirectly by acting as nuclei for cloud formation (Hemmilä, 2020; Kim et al., 2017; Oh et
41 al., 2020). Fine aerosol particles have sizes close to the wavelength range of the visible light, and therefore
42 they are expected to have a stronger climatic impact than larger particles (Kanakidou et al., 2005). In addition,
43 the aerosol particles also give an adverse effect on air quality and human health by exposing human's
44 respiratory system to aerosol particulate matter (PM) that can get into lungs and translocate into vital organs
45 due to their tiny size (Fu et al., 2013).

46 The formation and growth process of aerosol particles have been studied by many research groups (Ahlberg
47 et al., 2017; Camredon et al., 2007; Casquero-Vera et al., 2020; Kulmala et al., 2013, 2014; Peng et al., 2021;
48 Ziemann and Atkinson, 2012). To study the particle formation in the atmosphere, it is important to assess the
49 possible sources of the atmospheric particles, for instance by the presence of volatile organic compounds
50 (VOCs). Hydrocarbons and amines e.g. have been extensively investigated either by modelling or by
51 laboratory chamber experiments to show their contribution to secondary organic aerosol (SOA) formation.
52 These VOCs, along with other thousands of organic gaseous trace species, are directly emitted from biogenic
53 and anthropogenic sources. In the atmosphere, VOCs are oxidized by reactions with atmospheric oxidants
54 such as O_3^- , OH^- , NO_3^- and Cl^- radicals to form less volatile products and further subsequently partition into
55 aerosol particle leading to SOA formation (Almeida et al., 2013; Kulmala et al., 2014; Zahardis et al., 2008;
56 Ziemann and Atkinson, 2012). The SOAs then become the major components of fine aerosol particulate
57 matter, such as PM 10 and PM 2.5 that pollutes the environment (Fermo et al., 2021; Ge et al., 2011; Kulmala
58 et al., 2014).

59 Another important component that contributes to air pollution is Black Carbon (BC), which is emitted mostly
60 as a byproduct of fossil fuel combustion and biomass burning (Hyvärinen et al., 2011). In addition, industry,
61 energy production, and domestic cooking contribute to the BC in the atmosphere (Kumar et al., 2015). BC
62 has been associated with adverse effects on human health, such as premature mortality, and also on earth

63 temperature and climate, since it absorbs solar radiation very strongly (Anenberg et al., 2012; Jacobson,
64 2010).

65 In addition to VOCs and BC, atmospheric organic acids, such as low molecular weight (LMW) dicarboxylic
66 acids are also recognized as ubiquitous aerosol constituents in the urban region. As highly water-soluble
67 compounds they have the capability to significantly enhance the hygroscopicity of aerosol particles
68 (Kanakidou et al., 2005). LMW diacids can be emitted from biomass burning, vehicular exhausts, natural
69 marine, and also produced from the atmospheric photo-oxidation of various organic precursors (Fu et al.,
70 2013; Kawamura and Sakaguchi, 1999; Rinaldi et al., 2011).

71 The condensation particle counters (CPC) are important devices for the measurement of aerosol number
72 concentrations and aerosol particle fluxes (McMurry, 2000; Kangasluoma and Attoui, 2019; Petäjä et al.,
73 2001). CPCs are commonly used in the ambient air quality monitoring to measure the number concentration
74 of airborne submicron particles with sizes down to a few nanometers (Asbach et al., 2017; Buzorius et al.,
75 1998). The conventional CPCs have generally not been used as portable devices due to their weight and size.
76 However, recently small CPCs are emerging and being deployed for example for vertical profiling on-board
77 drones (Kim et al., 2018; Carnerero et al., 2018), and other platforms (Petäjä et al., 2012).

78 In our previous research, we used reliable and versatile miniaturized air sampling (MAS) techniques, which
79 have many benefits for on-site sampling, such as small size, low sampling time, environmental friendliness,
80 easy operation and flexibility for practical applications and automation (Lan et al., 2020; Pusfitasari et al.,
81 2022; Ruiz-Jimenez et al., 2019). Solid-phase microextraction (SPME) Arrow and in-tube extraction (ITEX)
82 sampling systems have been successfully employed for the reliable collection of VOCs from ambient air
83 samples (Lan et al., 2019b, a; Pusfitasari et al., 2022). An exhaustive sampling technique ITEX sampling
84 system with large sorbent volume can be fully automated, and it provides continuous air sampling, reliable
85 analysis, and quantification (Lan et al., 2019a; Pusfitasari et al., 2022). As an active sampler, ITEX system
86 allows the simultaneous collection of gas and particle phase compounds. Extra sampling accessories,
87 including adsorbent trap and filter accessories together with ITEX have enhanced the selectivity of the
88 sampling system and allowed the ITEX to collect only gas phase (Pusfitasari et al., 2022). After sample
89 collection, the compounds were desorbed from the samplers, separated and detected by thermal desorption
90 (TD) gas chromatography-mass spectrometry (GC-MS).

91 In this study, the sampling of VOCs and measurement of total particle number concentration and Black
92 Carbon (BC) directly at various altitudes, from 50 to 400 m, were performed using an aerial drone as the
93 platform as in our previous research (Lan et al., 2021; Pusfitasari et al., 2022; Ruiz-Jimenez et al., 2019). The

94 sampling platform contained now up to four SPME Arrows and four ITEX units, with additional portable
95 commercial BC device for BC real-time measurement and a lab-made portable CPC for total particle number
96 observation. The compositions of different gas phase fractions collected both by SPME Arrow and ITEX
97 systems, aerosol particles collected by ITEX sampling including filter accessory as well as BC and particle
98 numbers were evaluated at different altitudes and temporal variation at boreal forest SMEAR II Station in
99 October 2021. In addition, the possible correlation between VOCs, BC and total particle number
100 concentrations were also clarified.

101 **2. Materials and methods**

102 **2.1. Reagent and materials**

103 Detailed information of reagents used, including their purities, is given in the supplemental information S1.
104 Empty ITEX units, DVB-PDMS and Carbon coated WR-SPME Arrow systems were purchased from BGB
105 Analytik AG (Zurich, Switzerland). TENAX-GR was purchased from Altech (Deerfield, IL, USA). The
106 mesoporous silica-based materials, the Mobil Composition of Matter No. 41 (MCM-41) and titanium
107 hydrogen phosphate-modified (MCM-41-TP) materials were synthesized via sol-gel template as described
108 in our previous publication (Lan et al., 2019a). The instructions for ITEX packing with 30 mg MCM-41-TP
109 and 60 mg Tenax-GR are described in Lan *et al.* (2019b). The preparation of MCM-41-SPME Arrow with
110 the sorbent thickness of 40 μm and length of 20 mm, is found from Lan *et al.* (2019a).

111 **2.2. Instrumentation**

112 A lab-made permeation system was employed to create an artificial gas-phase sample in the laboratory (Lan
113 et al., 2019a, 2021; Pusfitasari et al., 2022). A PAL Cycle Composer and PAL RTC autosampler that were
114 used for sample collection and desorption in the laboratory were from CTC Analytics (Zwingen,
115 Switzerland). An Agilent 6890N gas chromatograph coupled with an Agilent 5975C mass spectrometer
116 (Agilent Technologies, Pittsburg, PA, USA) was used for the method optimization and quality assurance tests
117 for air samples in the laboratory. For onsite analysis, an Agilent 6890 N gas chromatograph (Agilent
118 Technologies, Pittsburg, PA, USA) equipped with a lab made ITEX heater for thermal desorption was
119 employed and coupled to an Agilent 5973 mass spectrometer. The GC capillary column used for the
120 chromatographic separations was an InertCap™ for amines (30 m length x 0.25 mm i.d., without any
121 information for the film thickness, GL Sciences, Tokyo, Japan).

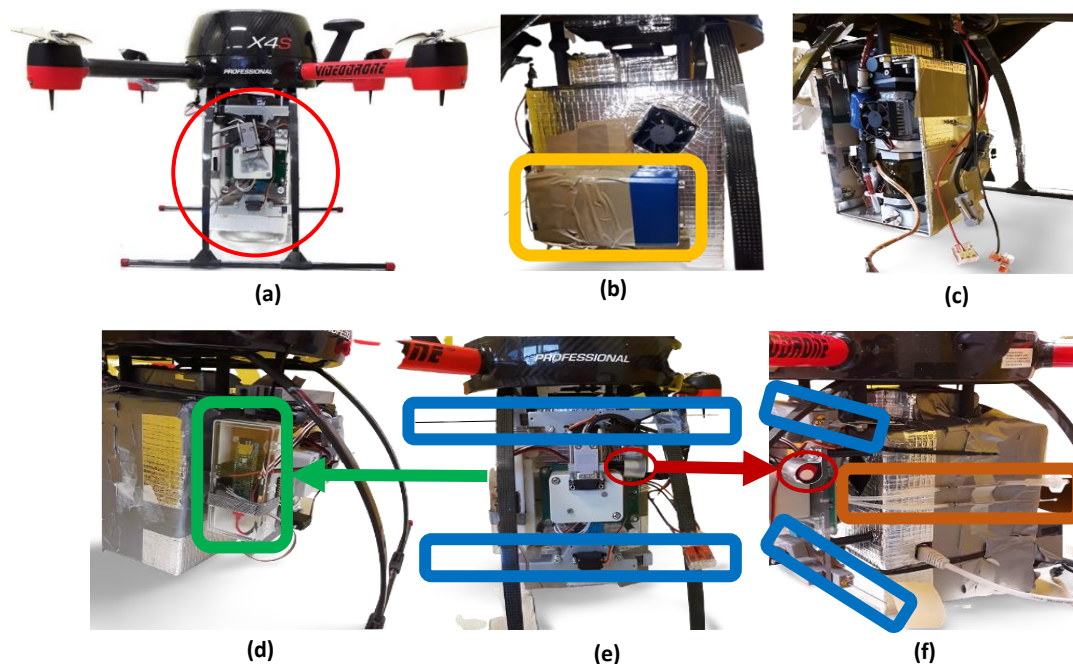
122 For organic acid determination, an Agilent 1260 Infinity high performance liquid chromatography (HPLC)
123 system equipped with a binary pump, autosampler, degassing unit, and a column compartment was employed
124 and coupled to an Agilent 6420 triple-quadrupole mass spectrometer with electrospray ion source (ESI)

125 (Agilent Technologies, Palo Alto, CA, USA). Chromatographic separations were performed with a 2.1x150
126 mm SeQuant[®]ZIC[®]-cHILIC (3 μm particle size) hydrophilic interaction liquid chromatography (HILIC)
127 column (MerckKGaA, Darmstadt, Germany). A KrudKatcher ULTRA HPLC in-line filter (0.5 μm) from
128 Phenomenex Inc (Torrance, CA, USA) protected the column from particulate impurities.

129 2.3. Drone platform construction

130 A remote-controlled Geodrone X4L (Videodrone, Finland), similar to that used in our previous studies (Lan
131 et al., 2021; Pusfitasari et al., 2022) with some modifications, was employed to carry out miniaturized air
132 sampling and analysis systems. With the dimension of 58x58x37 cm (width x depth x height), it could carry
133 the modified sampling box including our MAS system (up to four SPME Arrow units and up to four ITEXs)
134 with a new, light sampling pump for ITEX system. In addition, some portable devices were also attached to
135 the drone to measure Black Carbon (BC) and particle sizes by condensation particle counter (CPC). BC
136 portable device in the field was an AethLabs AE51-S6-1408, with the application version of 2.2.4.0 (San
137 Francisco, CA, USA). It was operated at 880 nm wavelength, with the air flowrate of 99 mL/min. The
138 portable CPC was a laboratory-made. The portable CPC measured total aerosol particle number concentration
139 between sizes from 20 nm and 5 μm. The references for BC and particle concentrations were measured at
140 Boreal forest SMEAR II Station at the altitude of 4 meters by an AE33 (operated at 880 nm) and an aerosol
141 electrometer (TSI 3772), respectively.

142



143

144 **Figure 1.** Drone platform sampling system with: (a) Air sampling box carried by aerial drone. (b) BC placed
145 behind the box. (c) CPC inserted into the sampling box. (d) The right side of the sampling box is a sensor
146 that measured temperature and relative humidity. (e) Front position of the sampling box consisted of SPME
147 Arrow units (marked with blue) and a VOC sensor (red circle). (f) Sides of the sampling box included ITEX
148 unit and filter accessory (brown).

149 2.4. Gas chromatography-mass spectrometry analysis

150 The SPME Arrow and ITEX sampling systems were preconditioned at 250 °C for 10 min under inert gas N₂.
151 Prior to sampling, decafluorobiphenyl vapor (as an internal standard) was spiked to SPME Arrow and ITEX
152 for 1 min and 5 mL, respectively. After sampling, the SPME Arrow unit was injected to the GC inlet to
153 desorb the analytes at the temperature of 250 °C for 1 min. While for ITEX, 800 µL of He was aspirated to
154 the ITEX syringe, and the analytes were desorbed at the temperature of 250°C and injected into the GC-MS
155 system by moving the plunger down with the injection speed of 200 µL s⁻¹. All the analyses were done in
156 splitless injection at 250 °C. For chromatographic separations, the GC oven temperature was programmed
157 from 40 °C (held for 2 min) to 250 °C (held for 10 min) at a rate of 20 °C min⁻¹. The temperature of transfer
158 line, ion source and quadrupole were 250, 230 and 150 °C, respectively. Electron ionization (EI) mode (70
159 eV) was used, and the scan range was from m/z 15 to 350. Helium (99.996 %, AGA, Espoo, Finland) was
160 used as a carrier gas at a constant flow rate of 1.2 mL min⁻¹.

161 2.5. Hydrophilic Interaction liquid chromatography-tandem mass spectrometry method for organic 162 acids analysis

163 Acetonitrile (ACN) was used as the main organic solvent containing 0.01 % formic acid (FA) (as Eluent A),
164 while Eluent B is aqueous 0.01 % FA solution. The applied LC gradient was the following: 5 % B (0-6 min),
165 5 to 20 % B (5-18 min), and post run for 15 min. The flow rate for the analysis was 0.25 mL min⁻¹ and column
166 temperature was maintained at 40 °C. The injection volume was 10 µl. The LC system was coupled to the
167 triple quadrupole mass spectrometer equipped with ESI. The ion source was operated in both positive and
168 negative modes.

169 2.6. Method development, quality control and quality assurance studies.

170 The optimization study for MCM-41-TP-ITEX system, including optimization of the adsorption and
171 desorption processes, sampling kinetics, breakthrough volume, and the recovery of the storage time, has been
172 carried out in our previous study using multivariate analysis (Pusfitasari et al., 2022). The evaluation and

173 validation of SPME Arrow units coated with MCM-41, DVB-PDMS, and carbon wide range (Carbon WR)
174 for the sampling of VOCs have also been studied in our previous research (Helin et al., 2015; Lan et al.,
175 2019b).

176 For TENAX-GR-ITEX sampler, the same method development and validation including the determination
177 of optimum flow rate, repeatability, reproducibility, and sample storage were done by using our laboratory-
178 made autosampler. The repeatability and reproducibility of TENAX-GR-ITEX system were studied by
179 analyzing the model compounds with five different ITEX units five times, each. The sampling flow rate (47
180 mL min⁻¹) was measured at least once for each ITEX during the comparison.

181 The storage study was performed by keeping the TENAX-GR-ITEX system at room temperature and in a
182 freezer (-20 °C). The purpose was to monitor how conditions affect the adsorption of chemicals in
183 surrounding environment to TENAX-GR during storage. The retainment of adsorbed analytes in different
184 conditions was also monitored. The difference in recovery between control sample (not stored) and stored
185 sample was regarded as the loss of the compound.

186 2.7. Application, measurement sites and sample collection in the field

187 The field sampling was carried out at the SMEAR II Station (Station for Measuring Ecosystem–Atmosphere
188 Relations; (Hari and Kulmala, 2005), with the coordinate of 61.84263° N - 24.29013° E), Hyytiälä, from 4 to
189 14 October 2021. As many as 53 drone flights were performed and 135 air samples in total were collected
190 (67 samples were collected using ITEX and 68 using SPME Arrow sampling systems). Table 1 shows the
191 summary of sampling and measurement techniques used in this study.

192 SPME Arrow units with different coating materials, DVB/PDMS, MCM-41, Carbon WR, were exploited to
193 collect gas phase samples. MCM-41-TP-ITEX and TENAX-GR-ITEX sampling systems were used to
194 simultaneously collect gas phase and particles. In the field study, the measured ITEX airflow ranged from 40
195 to 78 mL min⁻¹. The flow was carefully measured before the sampling and after analyte desorption. ITEX
196 sampling volumes were then obtained by multiplying the value of ITEX airflow rate with the sampling time.
197 Other sampling variables, such as sampling location, remained constant.

198 To study the average composition of VOCs in the atmosphere (Section 3.3), the samples were collected
199 simultaneously by ITEX and SPME Arrow systems located on the drone at the altitudes from 50 m to 400
200 m. Composition samples were collected for 2 min at each altitude and during the descending of the drone by
201 starting at the highest altitude of 400, followed by 300, 200, 100 and 50 m (Supplemental Fig. S1). In this

202 case, a total sampling time was 13-14 min (consist of total of 10 min at different altitudes, and 3-4 minutes
203 when the drone was descending from 400 m to 50 m), with a total flight time close to 20 min including take-
204 off and landing.

205 The VOC composition at the altitudes of 50 m and 400 m was also separately determined (Section 3.6). Detail
206 schematic picture on our sampling system is seen in the Supplemental Fig. S2 (sampling at 50 m for 10 min)
207 and Supplemental Fig. S3 (sampling at 400 m for 10 min).

208 Evaluation of ITEX sampling with filter accessory was also studied (Section 3.4). TENAX-GR-ITEX
209 furnished with filter accessory was employed to collect the gas phase only. A polytetrafluoroethylene (PTFE)
210 filter with the pore size of 0.2 μm (diameter of 13 mm, VWR) was used as ITEX filter accessory to remove
211 aerosol particles from the natural air samples. The results obtained were directly compared with those
212 achieved by Carbon WR-SPME Arrow sampling system. The recovery was calculated from the difference
213 between concentrations obtained by SPME Arrow and by ITEX furnished with filter accessory. Details about
214 the experiments, sampling time and altitudes are found from Supplemental Fig. S1.

215 Suitability of particle trap for subsequent analysis was evaluated by the determination of the organic acids
216 retained or adsorbed in the filter accessory (Section 3.5). Sample collection from drone at the altitude from
217 50 to 400 m is seen in Supplemental Fig. S4. Aerosol particles were collected onto the filter attached to ITEX
218 unit in the drone. All the collected samples were wrapped in aluminum foil and placed into separate Minigrip
219 bags which were stored in freezer (-20 °C) prior to analysis.

220 Portable BC and CPC devices were always active on measuring BC and total particle numbers during the fly
221 of the drone. The detected BC and total particle numbers obtained with our portable devices were then
222 compared with those obtained with reference devices at the SMEAR II Station (Section 3.7).

223 Table 1. Summary of target species, sampling and measurement techniques.

Target species	Sample phase	Sampler	Experiment(s)	Measurement technique
VOCs	Gas phase	ITEX + filter	Section 3.4	GC-MS
VOCs	Gas phase	SPME Arrow	Sec. 3.3; 3.4; and 3.6	GC-MS
VOCs	Particle phase	ITEX	Section 3.3 and 3.6	GC-MS
Carboxylic acids	Particle phase	Filter accessory	Section 3.5	HILIC-MS/MS
Black carbon	Particle phase	Portable AethLabs	Section 3.7	Real-time by Portable AethLabs
Total particle number	Particle phase	Portable CPC	Section 3.7	Real-time portable CPC

224

225 2.8. Data Processing and statistical analysis

226 Agilent ChemStation and Agilent Mass Hunter software were exploited for basic data processing, such as
227 peak identification and integration. An Mzmine2 (version 2.53) software, consisting of an algorithm
228 Automated Data Analysis Pipeline (ADAP-GC) was used for pre-processing untargeted mass spectrometric
229 data for detection, deconvolution, and alignment of the chromatographic peaks in natural samples (Ruiz-
230 Jimenez et al., 2019; Lan et al., 2021; Pusfitasari et al., 2022). NIST2020 (NIST MS Search v.2.3) mass
231 spectral database was used to check and compare the mass spectra of the aligned peaks as well as their
232 retention indices. The identified compounds should have a spectral match of >800 and ± 45 as the maximum
233 difference between experimental and library Kováts retention indices.

234 Partial least squares regression (PLSR) equations were developed for the quantification and semi-
235 quantification of the detected compounds in natural air samples (Kopperi et al., 2013; Lan et al., 2021;
236 Pusfitasari et al., 2022). To develop different PLSR equations for the quantification/semiquantification of
237 potentially identified compounds, six different concentration levels of 19 detected compounds, i.e. pyridine,
238 sec-butylamine, 1-butanamine, butanenitrile, 2-propen-1-amine, diethylamine, dimethylformamide,
239 hexylamine, trimethylamine, nonane, isobutanol, ethylacetate, methyl isobutyl ketone, hexanal, 2,3-
240 butanedione, benzaldehyde, acetophenone, p-cymene and ethyl benzene, were collected and analyzed under
241 optimal experimental conditions. Afterwards, the data was used for the development of the PLSR equation.

242 Total particle numbers measured by the reference instrument, an aerosol electrometer TSI 3772 at the altitude
243 of 4 m (ground level), were downloaded directly from the SmartSMEAR open-access database:
244 <https://smear.avaa.csc.fi/> (Junninen et al., 2009).

245 The measured VOC values that were collected by ITEX sampling system, and BC as well as total particle
246 numbers at different altitudes were calculated to the same pressure level so that they could be compared to
247 literature values (Brasseur et al., 1999; Kivekäs et al., 2009; Rajesh and Ramachandran, 2018). In this study,
248 the reading values were corrected for ambient pressure and temperature as the following:

$$249 \quad A = m_A \left[\frac{P_0 T}{P T_0} \right]^{-1} \quad (1)$$

250 where A is the corrected value, m_a is the measured raw concentration, P_0 is the standard atmospheric pressure
251 (101.3 kPa), T_0 is the standard temperature (293 K), P is the ambient atmospheric pressure, and T is the
252 ambient temperature. Supplemental Table S1 shows the data at ambient temperatures and pressures used in
253 this study, as well as the calculated correction factors at different altitudes. In the case of VOC concentrations

254 collected by SPME Arrows, no correction was applied since the equilibrium constant for current adsorbents
255 and compounds was not studied at various pressures and temperatures.

256 **3. Results and Discussion**

257 **3.1. Optimization of the sampling techniques using gas chromatography-mass spectrometry**

258 The choice of coating materials for SPME Arrow sampling systems was based on the good selectivity of
259 MCM-41 for nitrogen-containing compounds, suitability of DVB/PDMS for most of the VOCs present in the
260 air samples, and the capability of Carbon WR to collect volatile compounds, covers a wide range of polarity
261 and have a good reproducibility (Kim et al., 2020; Lan et al., 2019b; Ruiz-Jimenez et al., 2019). Whereas for
262 ITEX sampling system, the MCM-41-TP was chosen as a sorbent material since it has proved to have good
263 selectivity towards nitrogen-containing compounds, while TENAX-GR was selected due to its good
264 capability to collect different VOCs present in the air (Lan et al., 2019a; Pusfitasari et al., 2022).

265 The optimization containing equilibrium sampling time for SPME Arrow sampling systems, breakthrough
266 volume for MCM-41-TP-ITEX, desorption temperature and desorption time towards representative
267 compounds such as diethylamine, isobutylamine, triethylamine, trimethylamine, pyridine, p-cymene, 2-
268 butanol and 2-butanone have been tested in our previous studies (Pusfitasari et al., 2022). Briefly, the average
269 sampling time that is used before reaching equilibrium for both MCM-41-SPME Arrow and DVB/PDMS-
270 SPME Arrow units is about 20 min. The cleaning and desorption temperature of 250 °C for 10 min and 1
271 min, respectively, were selected to be optimal for the conditioning and analysis. The Carbon WR-SPME
272 Arrow sampling system was also treated in the same way in terms of conditioning and desorption methods.

273 In our previous study, TENAX GR as the sorbent for ITEX's trap-accessory was able to adsorb mostly non-
274 nitrogen containing compounds and only a small amount of nitrogen containing compounds (Pusfitasari et
275 al., 2022). In the present study, universal TENAX-GR was used as ITEX sorbent material to collect air
276 samples. Desorption and conditioning processes were optimized using a previously developed methodology
277 and optimal conditions similar to MCM-41-TP-ITEX system with selective sorbent (section 2.4). The
278 repeatability of TENAX-GR-ITEX sampler was also tested, with the RSD between 3.4 and 7.1 %
279 (Supplemental Tables S2 and S3), whereas the reproducibility between different ITEX units caused also by
280 ITEX manual packing was between 4 and 18 %.

281 The sampling systems used in this study needed to be stored for a certain period of time before analysis to
282 accommodate the on-field situation. In our previous study, the sorbent in MCM-41-TP ITEX system could
283 be stored at -20 °C up to 18 h without losing much of the model compounds, with the recoveries of around

284 80 % (Pusfitasari et al, 2021). For TENAX-GR sorbent, the recoveries of 98 % were obtained after storage
285 at $-20\text{ }^{\circ}\text{C}$ for 24 h, but only 78 % when the sorbent was stored at room temperature for 24 h. In this study,
286 the samples collected at the SMEAR II Station had to be analysed after storage of around 2 hours since the
287 samplers were needed for the upcoming field measurements. Therefore, both MCM-41-TP- and TENAX-
288 GR-ITEX systems were stored at room temperature only for a few hours before the analysis.

289 **3.2. Optimization of organic acid analysis using hydrophilic interaction liquid chromatography** 290 **(HILIC)- tandem mass-spectrometry**

291 HILIC-ESI-MS/MS was employed for analysis of organic acid from filter samples. 18 different acids were
292 successfully identified and five of them were quantified using the optimized method. For the 18 model acids,
293 HILIC mobile phase with composition of ACN 80 % (solvent A) and 20 % of 0.005 % FA (solvent B) was
294 chosen as the best eluent for acids separation (Supplemental Table S4). The second optimized parameter was
295 drying gas temperature which is important parameter in the ESI technique to allow the eluent from the HILIC
296 column to evaporate as rapidly as possible in the ion source (Kruve, 2016). In this study, using the selected
297 optimum eluent, i.e. ACN (80 %) and 0.005 % FA (20 %), with the flow rate of 0.25 mL min^{-1} , the drying
298 gas temperature of $275\text{ }^{\circ}\text{C}$ was selected as the optimum temperature. Supplemental Table S5 shows the
299 established multiple reaction monitoring (MRM) method parameters for each compound using all optimized
300 parameters including the optimized voltages for other crucial parameters, namely fragmentor voltage,
301 collision energy and cell acceleration voltage (CAV).

302 **3.3. Application of air sampling system at the altitude from 50 to 400 m**

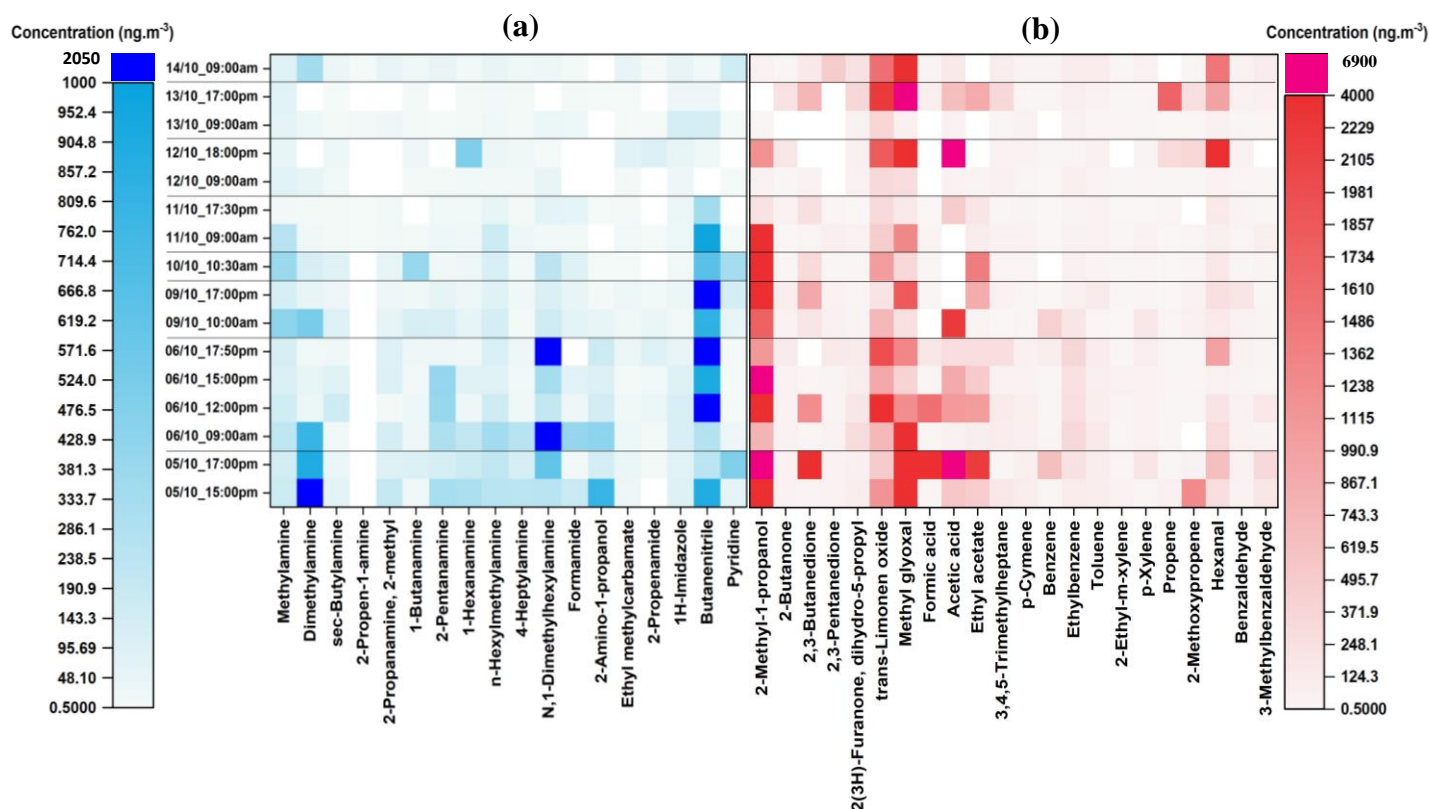
303 In this study, the mesoporous silica-based materials, namely MCM-41 and MCM-41-TP, were used to
304 selectively collect nitrogen-containing compounds (Lan et al., 2019b; Pusfitasari et al., 2022). Whereas the
305 commercial universal materials, TENAX-GR and DVB/PDMS were also used to collect other than nitrogen-
306 containing compounds.

307 MCM-41-TP-ITEX and TENAX-GR-ITEX sampling systems were used to collect atmospheric air samples
308 containing both gas phase and aerosol particles, while the samples containing only gas-phase were collected
309 by MCM-41-SPME Arrow and DVB/PDMS-SPME Arrow systems. The concentrations in aerosol particles
310 were obtained via the subtraction of these results, i.e. MCM-41-TP-ITEX subtracted with MCM-41-SPME
311 Arrow, and TENAX-GR-ITEX subtracted with the DVB/PDMS-SPME Arrow.

312 Altogether, up to 40 VOCs were detected in gas phase and 48 were in particle phase samples. VOCs with
313 various functional groups such as nitrogen-containing compounds, alcohols, ketones, aldehydes, small

314 organic acids, and hydrocarbons were detected both by selective MCM-41 coated SPME Arrow and MCM-
 315 41-TP-ITEX sampling systems and by universal sorbent materials TENAX-GR-ITEX and DVB/PDMS
 316 coated SPME Arrow systems. However, because in our previous study (Lan et al., 2019b; Pusfitasari et al.,
 317 2022), the MCM-41-SPME Arrow and MCM-41-TP-ITEX samplers gave sensitive and reliable results in
 318 collecting selectively nitrogen-containing compounds, only the results obtained by MCM-41-SPME Arrow and MCM-
 319 41-TP-ITEX samplers are shown for nitrogen-containing compounds in this section. While data for other
 320 VOCs were collected using ITEX with universal sorbent materials TENAX-GR and using DVB/PDMS
 321 coated SPME Arrow.

322

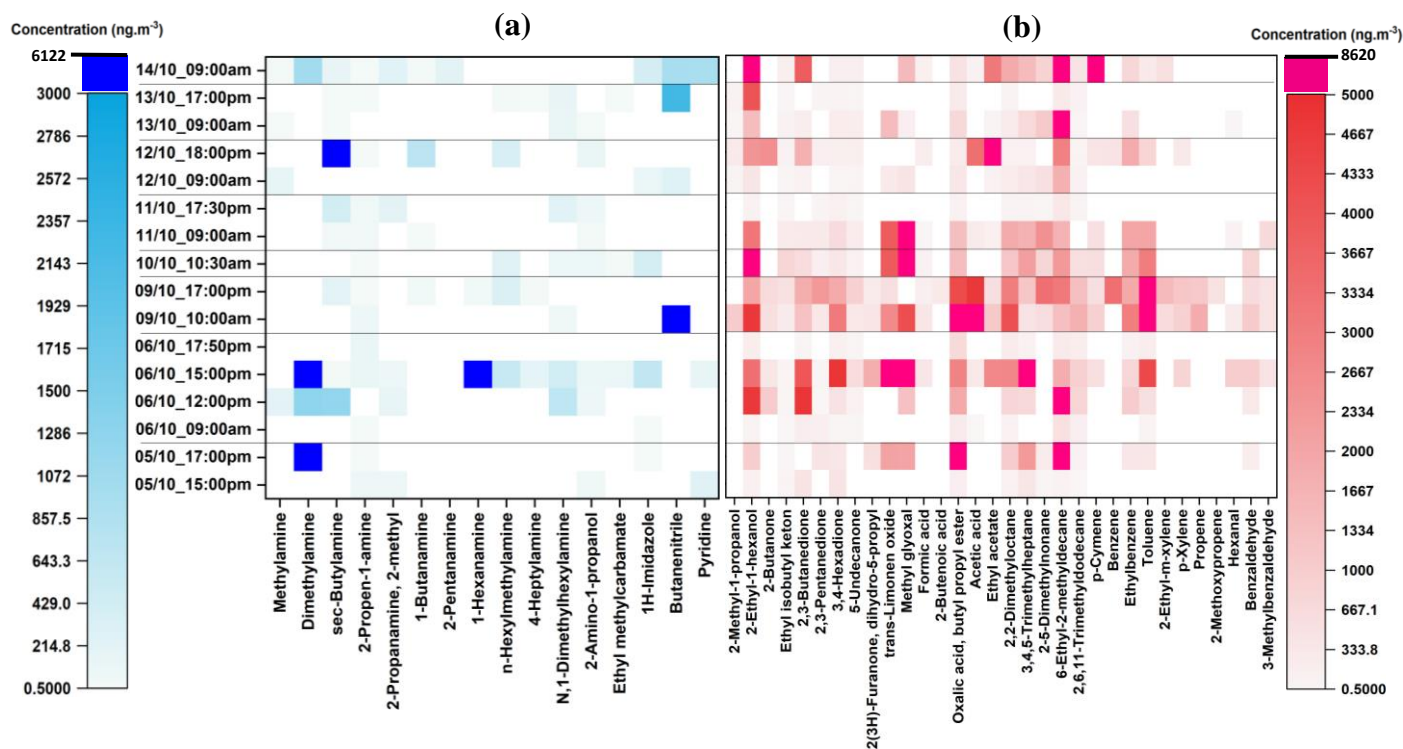


323

324 **Figure 2.** Concentrations of (a) nitrogen-containing compounds and (b) other VOCs in the gas-phase at the
 325 SMEAR II Station, Hyytiälä at the mixed altitude between 50 and 400 m. (a) Nitrogen-containing compounds
 326 were collected using MCM-41-SPME Arrow system with selective sorbent, while (b) other VOCs were
 327 collected using DVB/PDMS-SPME Arrow system with universal sorbent. White color = not detected.

328

329



330

331 **Figure 3.** Concentrations of **(a)** nitrogen-containing compounds and **(b)** other VOCs in the particle phase at
 332 SMEAR II Station, Hyytiälä at the mixed altitude between 50 and 400 m. Samples were collected using
 333 MCM-41-TP-ITEX system with selective sorbent **(a)** and TENAX-GR-ITEX systems with universal sorbent
 334 **(b)**. White color = not detected.

335 As can be seen from Fig. 2, eleven aliphatic amines (methylamine, dimethylamine, sec-butylamine; 2-
 336 propen-1-amine; 2-methyl-2propanamine; 1-butanamine, 2-pentanamine, 1-hexanamine, n-
 337 hexylmethylamine, 4-heptylamine, N,1-dimethylhexylamine) and seven other nitrogen-containing
 338 compounds (formamide, 2-amino-1-propanol, ethylmethylcarbamate, 2-propenamide, 1H-imidazole,
 339 butanenitrile, and pyridine) were detected, quantified and semi quantified in gas phase samples with the
 340 concentrations up to 2005 ng m⁻³. While in the particle phase (Fig. 3), the total of 16 nitrogen-containing
 341 compounds was detected with the concentrations up to 6122 ng m⁻³. These results are comparable to our
 342 previous study in which the concentrations of nitrogen-containing compounds were up to 2930 ng m⁻³ and
 343 5480 ng m⁻³ in gas phase and particle phase, respectively (Pusfitasari et al., 2022). However, the samples
 344 were collected then at the altitude from 50 to 150 m (Pusfitasari et al., 2022).

345 Dimethylamine, that can be produced by animal husbandry, cattle, landfill, sewage, and also industry (Ge et
 346 al., 2011), was detected in both gas and particle phase during afternoon with the concentrations up to 1004
 347 ng m⁻³ for gas phase, and up to 5909 ng m⁻³ for the particle phase (Fig. 2a and Fig. 3a). Studies have indicated

348 that organic amines, including DMA, can be present to large extent in the particles e.g. by transferring from
349 gas phase to particles (Chen et al., 2022; Zhao et al., 2007; Yu et al., 2017). DMA is one of the most common
350 and abundant amines found in the atmosphere, and particulate DMA concentrations can increase due to
351 enhanced BVOC emissions and due to aerosol-phase water that increase their partition to the condensed
352 phases (Ge et al., 2011; Youn et al., 2015; Chen et al., 2017).

353 Other amines that were detected at high concentrations were methylamine, pentanamine, hexanamine,
354 hexylmethylamine, and dimethylhexylamine with the concentrations up to 432, 395, 493, 340, and 1393 ng
355 m⁻³, respectively (Fig. 2a). For the particles, sec-butylamine was detected with the concentrations up to 4090
356 ng m⁻³, hexanamine up to 4316 ng m⁻³ and dimethylhexylamine up to 686 ng m⁻³ (Fig. 3a).

357 For nitrogen-containing compounds other than amine, butanenitrile was detected as the highest
358 concentrations up to 2005 ng m⁻³ in gas and 6122 ng m⁻³ in particle phases. 2-Amino-1-propanol, pyridine,
359 and 1-H-imidazole were present in gas phase as the second, third and fourth highest concentrations up to 790,
360 492, and 136 ng m⁻³, respectively. While in the particle phase, their concentrations were up to 129, 958, and
361 646 ng m⁻³, respectively. The concentrations of all detected nitrogen-containing compounds at mixed
362 altitudes can be seen in Supplemental Table S7.

363 For other VOCs, 22 compounds in gas phase (Fig. 2b) and 32 in particle phase (Fig. 3b), containing alcohols,
364 aldehydes, ketones, small organic acids and hydrocarbons were detected and quantified or semi quantified
365 with the concentrations up to 6898 ng m⁻³ in the gas phase and 8613 ng m⁻³ in the particle phase. In the gas
366 phase, 2-methyl-1-propanol; 2,3-butanedione; trans-limonene oxide, methylglyoxal, acetic acid, ethyl
367 acetate, and hexanal were discovered almost all the time during the samplings with the concentration up to
368 4209, 2436, 2210, 4695, 6898, 2198 and 3984 ng m⁻³, respectively (Fig. 2b). While in the particle phase,
369 almost all detected compounds were present in high concentrations such as 2-ethyl-1-hexanol (4114 ng m⁻³);
370 2,3-butanedione (4865 ng m⁻³), trans-limonene oxide (6886 ng m⁻³), methylglyoxal (8613 ng m⁻³), aliphatic
371 hydrocarbons (7091 ng m⁻³), ethyl benzene (3042 ng m⁻³) and toluene (7715 ng m⁻³), (Fig. 3b). Supplemental
372 Table S8 gives at mixed altitudes (50 to 400 m) the concentrations for all detected VOCs that do not belong
373 to nitrogen-containing compounds.

374 In the atmosphere, 2,3-Butanedione is naturally occurring in food products such as butter and beers (Boylstein
375 et al., 2006), while trans-limonene oxide is detected possibly due to the partial oxidation of monoterpene
376 limonene's olefinic bonds (Hoeben et al., 2012; Karlberg et al., 1992). Methylglyoxal, an important precursor
377 of SOA, is produced in the atmosphere by the oxidation of hydrocarbons, such as isoprene, acetylene, toluene,
378 and xylenes (Zhang et al., 2016; Fu et al., 2013; Olsen et al., 2007). Other detected compounds, e.g. acetic

379 acid and ethyl acetate can be released from different sources such as biomass burning and vegetation
380 (Rosado-Reyes and Francisco, 2006; Khare et al., 1999).

381 The diurnal pattern in both gas and particle-phases was also observed. As can be seen from Fig. 2 in the gas
382 phase, aliphatic amines that are mostly emitted by biogenic sources were present in lower concentrations in
383 the evening (started at 17:00 pm) compared to daytime, whereas some amines, namely hexanamine and
384 dimethylhexylamine, had slightly higher concentrations in the evening. These results agree well with our
385 previous study in which most of the amines had a diurnal variation with a daytime maximum due to their
386 dependency on temperature for their emission, indicating the contribution to biogenic sources (Pusfitasari et
387 al., 2022). High concentrations of some amines in the evenings could be caused by the weak atmospheric
388 mixing at night resulting in decreased reactions with atmospheric acids (Hemmilä et al., 2018). In contrast,
389 VOCs that were emitted from other sources had higher concentrations mostly in the afternoons, except for
390 non-nitrogenated compounds with high concentrations also in the mornings on 11 October 2021. The
391 anthropogenic sources that might affect this result, were probably carried by the wind from other places and
392 were mixed in the atmosphere since the samples were collected at high altitudes (up to 400 m). In the particle
393 phase, there was no clear pattern seen since our samples were mostly collected only in the mornings and late
394 afternoons. However, in our previous study we found that VOCs had high concentrations in mornings and
395 evenings since temperature dependency affects the deposition of amines in the colder evenings, and then they
396 partition back to the atmosphere in the higher temperature mornings (Pusfitasari et al., 2022). In this present
397 study we can also see from Fig. 3 high concentrations both in the mornings and late afternoons, but
398 surprisingly also at noon (on 6 October).

399 The correlation among all the VOCs in both gas and particle phases was also studied. R-value close to one
400 and P-value <0.05 mean that there is correlation between variables. As can be seen from Supplemental Fig.
401 S5, only a few compounds in gas phase correlate with those detected in the particle phase, such as particulate
402 benzaldehyde that correlated with alcohol vapors (i.e. gas-phase of 2-methyl-1-propanol and 2-ethyl-1-
403 hexanol) and some amines (i.e. methylamine, sec-butylamine, 2-pentanamine, and n-hexylmethylamine).
404 These correlations can be explained by the studies conducted by Perez et al (2017) who was investigating the
405 implication of aldehyde – amines to the aerosol growth by providing low-energy neutral pathways for the
406 formation of larger and less volatile compounds (Perez et al., 2017).

407 In addition, we can also see that some nitrogen-containing compounds correlated with aliphatic
408 hydrocarbons, aliphatic carbonyl, and aliphatic alcohols in the gas phase, indicating that they might be
409 emitted from the same sources. This finding is supported by the study conducted by Isidorov *et al* (2021).
410 Although their group could not detect selectively nitrogen-containing compounds because they used

411 universal sorbent material for the collection of air sample (i.e. DVB/CAR/PDMS-SPME), they could detect
412 all other VOCs compounds at the same time from the boreal forest (Isidorov et al., 2022).

413 **3.4. Evaluation of ITEX filter accessories**

414 In our previous study, it was proved that a small filter can be used to trap particles allowing only gas phase
415 enter the ITEX sampler (Pusfitasari et al., 2022; Ruiz-Jimenez et al., 2019). The experiments were properly
416 designed to check and compare the results achieved for gas phase compounds using a passive SPME Arrow
417 and an active ITEX + filter sampling systems. In the present study, the samples were collected from 11 to 14
418 October 2021 and TENAX-GR-ITEX was exploited with the filter accessory. The altitudes for these
419 experiments were 50-400 m (Supplemental Fig. S1). As can be seen in Supplemental Fig. S6, aliphatic amines
420 were the major nitrogen-containing compounds detected both in the gas and particle phases. For VOCs
421 without any nitrogen compounds, following the results in the previous section (i.e. section 3.3.), alcohols,
422 ketones, aldehydes, organic acids and some hydrocarbons were detected, quantified and semiquantified with
423 the concentrations shown in Supplemental Fig. S6. The results of the gas-phase sampled by ITEX system
424 with filter accessory were comparable with the gas phase results obtained by the SMPE Arrow sampling
425 system.

426 In addition to the comparison of gas phase collected by ITEX furnished with filter accessory and by SPME
427 Arrow system, the compound recoveries of gas phase obtained by the first sampling system ITEX furnished
428 with filter were also evaluated. The recoveries of non-polar compounds, such as alkanes, were only <50 %
429 (Supplemental Table S9). The more polar compounds, such as alcohols, acids, and nitrogen-containing
430 compounds, were mostly detected at higher recoveries from 50 % up to 99 %. Most probably non-polar
431 compounds of the gas phase were partly adsorbed to the ITEX filter accessory that was made from PTFE
432 (Parshintsev et al., 2011). PTFE has a non-polar structure due to the distribution of the fluorine atom around
433 the carbon polymer backbone which balances the electronegative and electropositive charges (Parsons et al.,
434 1992). Hence, our study proved that ITEX with PTFE filter does not only trap aerosol particles but is also
435 excellent for the collection of polar compounds, such as nitrogen-containing compounds, of gas phase.
436 Nevertheless, since nitrogen-containing compounds are very water soluble, the humidity level in the air will
437 most likely affect the distribution of polar compounds between the filter and ITEX adsorbent, e.g. water
438 condensing to the filter at high humidity.

439 **3.5. Analysis of aerosol particles collected by ITEX with PTFE filter using liquid chromatography** 440 **tandem mass spectrometry**

441 Filter collecting aerosol particles in ITEX was extracted and analyzed separately by using HILIC-MS/MS to
 442 quantify carboxylic and dicarboxylic acids since most organic acids cannot be analyzed by GC without
 443 derivatization, except small organic acids such as formic acid and acetic acid. The organic acids have
 444 capability to significantly enhance the hygroscopicity of aerosol particles and contribute to the acidity of
 445 precipitation and cloud water.

446 As can be seen in Table 2, five main acids, succinic acid, benzoic acid, phthalic acid, glutaric acid, and adipic
 447 acid, were identified and quantified. Succinic acid was observed almost in every sample and its higher
 448 prevalence could possibly be explained by the fact that it can be formed from common biogenic and
 449 anthropogenic precursors such as isoprene and toluene (Sato et al., 2021). The aromatic acids such as benzoic
 450 acid and phthalic acid were also detected in the samples. The concentrations of benzoic acid (up to $1.4 \mu\text{g m}^{-3}$)
 451 ³) were higher than those of phthalic acid (up to $0.77 \mu\text{g m}^{-3}$). Observation of these acids is relevant as their
 452 aromatic hydrocarbon precursors are common in the atmosphere. In addition, phthalic acid has also been
 453 detected in the summer 2012 samples, but then no benzoic acid was detected in the gas phase or particulate
 454 phase (Kristensen et al., 2016).

455 **Table 2.** Concentrations of acids collected from the ITEX filters at the altitudes of 50-400 m.

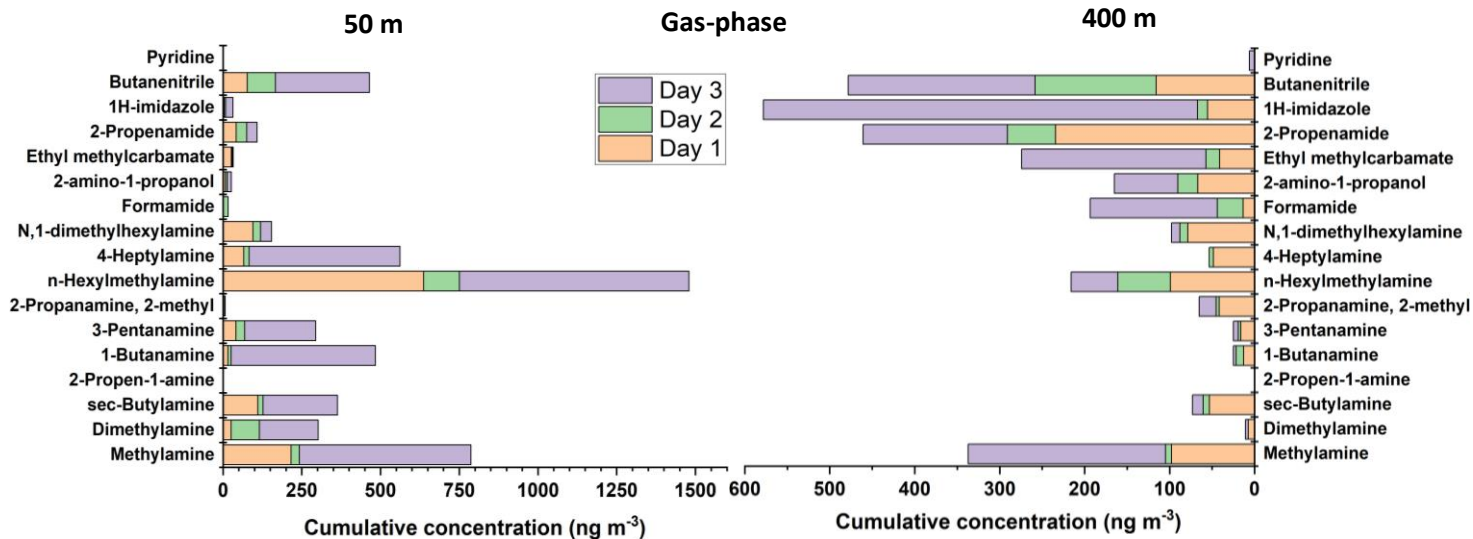
Sampling time	Succinic acid (ng m^{-3})	Benzoic acid (ng m^{-3})	Phthalic acid (ng m^{-3})	Glutaric acid (ng m^{-3})	Adipic acid (ng m^{-3})
11.10.2021	1416	1416	657	1619	10926
12.10.2021	435-789	1416	769	n.d.	n.d.
13.10.2021	496-4654	n.d.	n.d.	n.d.	n.d.
14.10.2021	n.d.	n.d.	n.d.	1720	6374

456 *n.d. = not detected

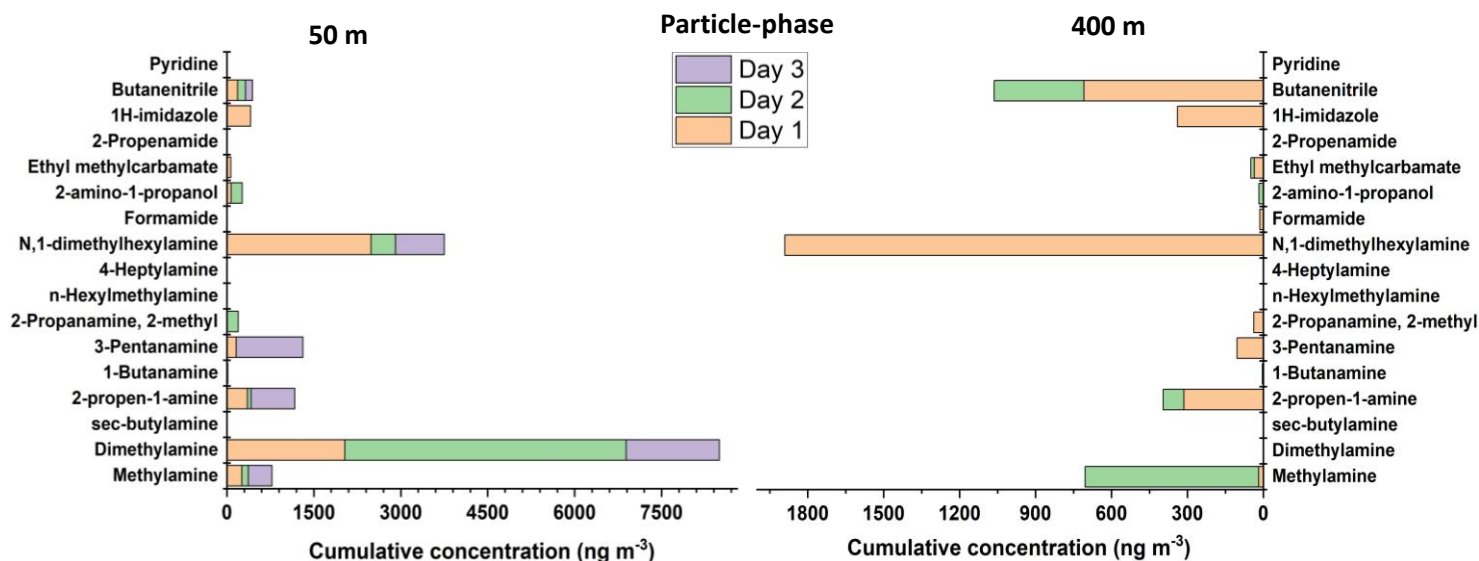
457 Glutaric and adipic acids were also determined from samples taken on the 11th and 14th of October. Glutaric
 458 acid and adipic acid have been commonly detected in atmospheric aerosols and cloud droplets (Wen et al.,
 459 2021). Other dicarboxylic acids, such as glycolic acid and cis-pinonic acid were detected in only one sample
 460 in which their LODs were exceeded (Supplemental Table S10). The possible reason for the low concentration
 461 of glycolic acid might be that it can be formed as an oxidation product of biogenic isoprene (Liu et al., 2012).

462 **3.6. Comparison of nitrogen-containing compounds and other VOCs at the altitudes of 50 m and 400** 463 **m**

464 The aim of this study was to compare the composition of VOCs at the altitudes of 50 m and 400 m, separately.
 465 Carbon WR-SPME Arrow unit with universal sorbent was used to collect a wide range of VOCs in the gas
 466 phase. MCM-41-TP-ITEX and TENAX-GR-ITEX sampling systems were employed to collect gas and
 467 particle phases.



469



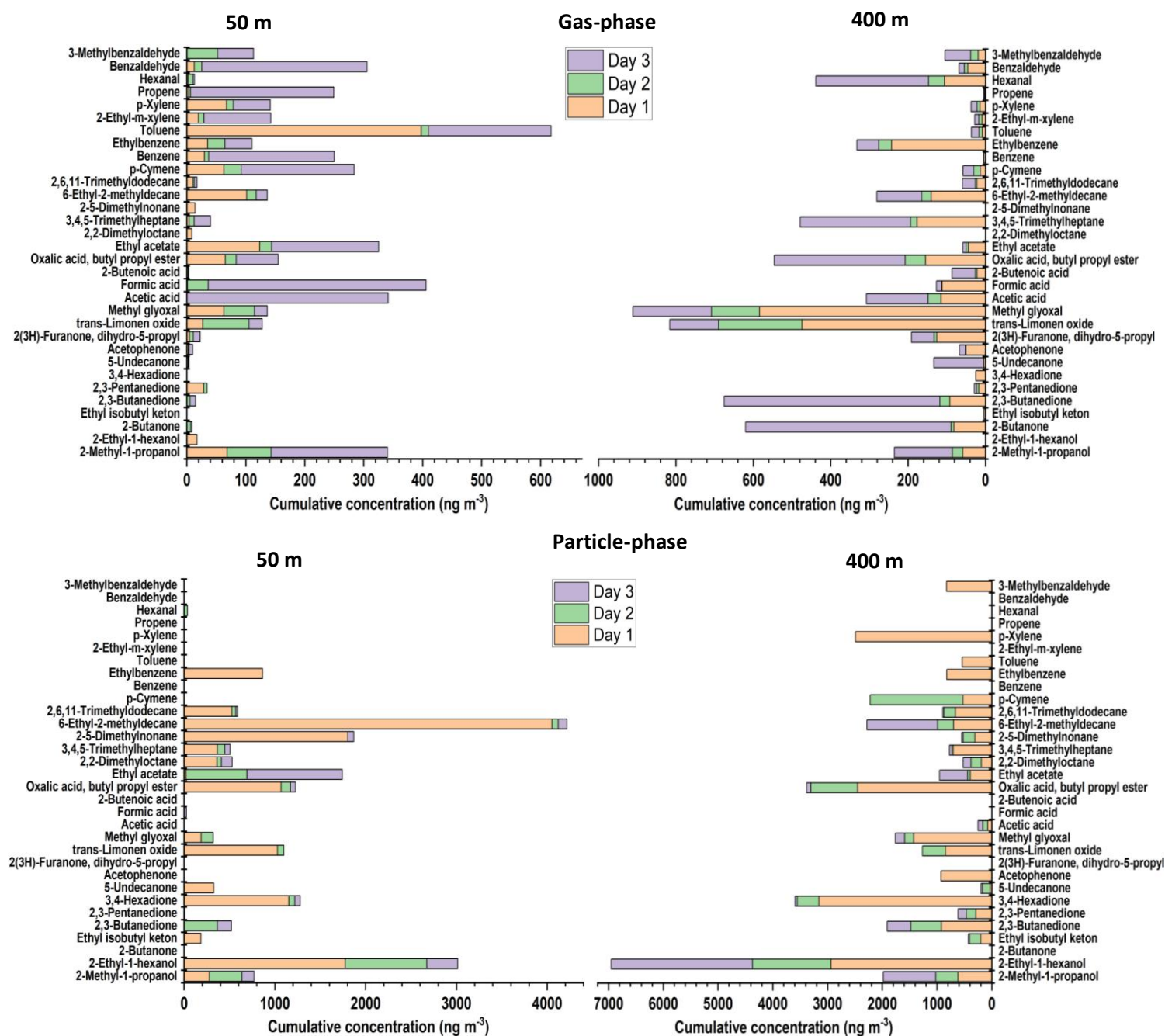
470 **Figure 4.** Concentrations of nitrogen-containing compounds in the gas-phase and in particle-phase at
 471 SMEAR II Station at altitudes 50 and 400 m for three days (8 to 10 October 2021). For the gas-phase samples
 472 were collected using Carbon WR-SPME Arrow sampling system, and the particle-phase samples were
 473 collected by MCM-41-TP-ITEX system. The concentrations of aerosol particle compounds were obtained
 474 via subtraction the results obtained by MCM-41-TP-ITEX from those obtained by Carbon WR-SPME Arrow
 475 with universal sorbent.

476 As can be seen from Fig. 4, the concentrations of amines that were emitted by biogenic sources, such as
 477 methylamine, dimethylamine, sec-butylamine, butanamine, pentanamine, hexylmethylamine, and
 478 heptylamine, were mostly found at higher concentrations at the lower altitude (50 m). The concentrations

479 were decreased at higher altitude 400 m most probably due to the dilution (since the sources are on the
480 ground) and reaction with hydroxyl radical (Kieloaho, 2017).

481 For nitrogen containing compounds, other than amines, imidazole was one of the compounds detected by our
482 system. There have been a number of laboratory studies where imidazole has been reported to be the major
483 product of glyoxal reaction with ammonium ions or primary amines on secondary organic aerosol. In
484 addition, imidazoles can become a secondary product of the reaction of dicarbonyls with nitrogen containing
485 compounds, therefore they might have potential to act as photosensitizers triggering secondary organic
486 aerosol growth and are forming constituents of light absorbing brown carbon (De Haan et al., 2011; Dou et
487 al., 2015; Teich et al., 2020). Imidazoles were detected mostly in the particle phase with concentrations up
488 to 422 ng m^{-3} at 50 m and 338 ng m^{-3} at 400 m. Slightly lower concentrations were discovered in the gas
489 phase with the values up to 58 ng m^{-3} at the altitudes of 50 m, and 510 ng m^{-3} at the altitude of 400 m.

490 Other nitrogen-containing gas phase compounds detected, such as formamide, 2-amino-1-propanol,
491 ethylmethylcarbamate, and propenamide showed also the same pattern with higher concentrations at 400 m
492 than at 50 m. These compounds were most probably transported by the wind from other areas and emitted by
493 various sources, such as biomass burning, peatland, industries, and other anthropogenic sources (Pusfitasari
494 et al., 2022).



496 **Figure 5.** Concentrations of non-nitrogenated VOC compounds in the gas-phase and in particle-phase at
 497 SMEAR II Station at altitudes 50 and 400 m for three days (8 to 10 October 2022). The gas-phase samples
 498 were collected using Carbon WR-SPME Arrow system, and particle-phase samples using TENAX-GR-ITEX
 499 sampling systems. The concentrations of aerosol particle compounds were obtained via subtraction the results
 500 obtained by TENAX-GR-ITEX from those obtained by Carbon WR-SPME Arrow with universal sorbent.

501 As can be seen from Fig. 5 gas-phase VOC compounds without nitrogen, such as trans-limonene oxide,
502 methylglyoxal, hexanal and ketones have higher concentrations at the altitude of 400 m compared to 50 m.
503 Whereas some acids, such as acetic acid and formic acid, ethyl acetate, and BTX (benzene, toluene, xylene)
504 were mostly discovered at the altitude of 50 m. In the case of alcohols, they had comparable concentrations
505 at both 50 and 400 m. In the particle phase, most of the compounds had higher concentrations at 400 m than
506 at 50 m, except for some hydrocarbons (such as 2,5-dimethylnonane and 6-ethyl-2-methyldecane) that had
507 high concentrations at 50 m.

508 Alcohols are a prevalent class of VOCs in the atmosphere and can be emitted by biogenic sources such as
509 rain forest, and also from anthropogenic sources such as alcohol-gasoline blended fuel and industries
510 (Nguyen et al., 2001; McGillen et al., 2017). Therefore, it is no wonder that in this study alcohol was found
511 almost in all altitudes. The alcohol emission is becoming concern since it can react with Criegee intermediates
512 (product of biogenic alkenes oxidized by ozone) to produce α -alkoxyalkyl hydroperoxides (AAAHs) that can
513 lead to the formation of secondary organic aerosols (Sahli, 1992; Bonn et al., 2004; McGillen et al., 2017).

514 In the gas phase samples, benzene, toluene, and p-xylene (BTX) were found mostly at the altitude of 50 m
515 with the concentrations up to 219, 410, and 70 ng m^{-3} , respectively. Since BTX can be emitted from the
516 gasoline (major fuel of vehicles) and the samples were collected close to the parking area, the higher
517 concentrations were found at lower altitude 50 m. This finding is comparable with the study conducted by
518 Chen et al (2018) who measured the BTX concentrations between 100 and 300 ng m^{-3} from forest canopy at
519 the altitude between 20 and 26 m (Chen et al., 2018; Yassaa et al., 2006). Toluene and p-xylene were also
520 detected in the particle phase as VOCs may be adsorbed onto the surface of the particles (Dehghani et al.,
521 2018; Kamens et al., 2011). The higher concentrations were detected at the altitude of 400 m with the
522 concentrations of up to 539 ng m^{-3} and 2475 ng m^{-3} for toluene and p-xylene, respectively. BTX play an
523 important role in the atmosphere since they have been recognized as important photochemical precursors for
524 the secondary organic aerosol (Correa et al., 2012; Ng et al., 2007).

525 Aldehydes in the atmosphere are also of concern because of their heterogeneous reaction with acids affecting
526 the particle growth (Jang and Kamens, 2001; Altshuller, 1993). In our study, some aldehydes, such as
527 methylglyoxal, hexanal and benzaldehyde, were found both in the gas and particle phase at the altitude of
528 400 m in higher concentrations than at the altitude of 50 m. At the altitude of 400 m, methylglyoxal was the
529 most abundant aldehyde with the concentrations up to 580 ng m^{-3} in the gas phase, and 1418 ng m^{-3} in the
530 particle phase. Ketones in aerosol particles have been associated with burning and non-burning forest, and it
531 represented up to 27 % of the current organic aerosol mass concentration (OM) (Takahama et al., 2011).

532 Ketones were also found in this study at higher concentrations at high altitude 400 m in both gas phase and
533 particle phase.

534 The last group of chemicals that was detected by our collection systems was small organic acids, and from
535 these especially formic acid and acetic acid. Organic acids have an important role as chemical constituent in
536 troposphere and they contribute with a large fraction (25 %) to the nonmethane hydrocarbons in the
537 atmosphere. The organic acids contribute to the acidity of precipitation and cloud water (Khare et al., 1999).
538 Acetic acid was found in both gas and particle phases at the altitudes of 50 and 400 m. However, the amount
539 of both formic acid and acetic acid found in the gas phase was higher than that in the particle phase. These
540 acids can originate from various sources such as vehicular emissions, ants, plants, soil, and biomass burning
541 (Zhang et al., 2022).

542 **3.7. Evaluation of total particle numbers and black carbon at high altitudes. Portable CPC and BC** 543 **devices carried by aerial drone**

544 The particle number concentration and BC concentration were measured by using portable CPC and BC
545 measurement devices carried by the drone. The BC concentration was measured at 880 nm wavelength (near
546 IR), as at this wavelength BC has strong absorption and least interferences by other organic molecules
547 (Dumka et al., 2010). The results were compared to those measured by the reference instruments at the
548 SMEAR II Station. The correction factors to the same pressure level as described in section 2.8 were
549 calculated with the values between 0.994 and 1.035 (Supplemental Table S1). Supplemental Figure S7 for
550 CPC proves a correlation between the results obtained by our portable CPC and reference instrument, with
551 direct linear close to 1 (R^2 of 0.9564). Oppositely, linear correlation for BC was only 0.2492, indicating that
552 there was no correlation between the reference instruments and our BC meter in the drone.

553 Our portable BC monitor in the drone gave higher concentration values than the reference one, located at 4
554 m. The reasons for the differences could be caused by amplification factor that raised due to multiple
555 scattering in quartz fiber matrix of the tape of the Aethalometer. The deposition of scattering material along
556 with BC to the filter tape produced the “shadowing effect” causing the BC meter to show higher concentration
557 values (Weingartner et al., 2003; Dumka et al., 2010). Alternatively, the differences can be explained by
558 different measurement altitudes between the reference instrument (measured at 4 m) and BC monitor in the
559 drone (up to 400 m). At lower altitude, living activities such as heating sauna and fuel burning from cars
560 nearby the area might contribute to the results, while at higher altitudes BC long distance transport contributes
561 to the results as well (Meena et al., 2021). The atmospheric boundary layer height (ABLH) also plays an
562 important role to govern concentration of BC at high altitudes since it can affect pollutant aggregation,

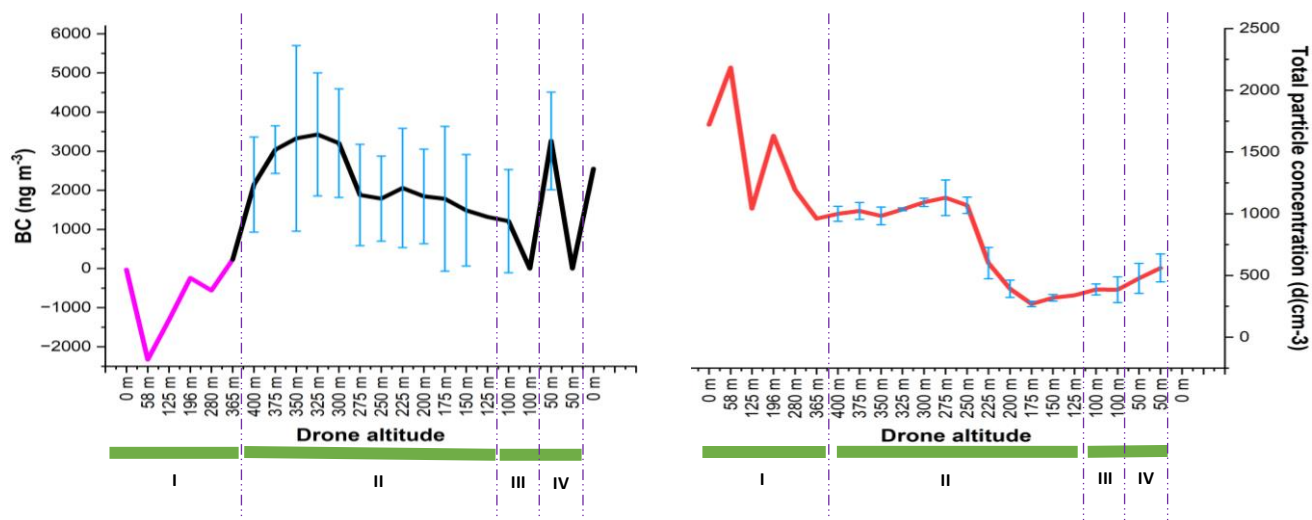
563 transmission, wet deposition, and dry sedimentation (Meena et al., 2021). The boundary layer (BL) is the
 564 lowest part of troposphere and connects the ground and the free atmosphere. The average boundary layer
 565 height at Hyytiälä SMEAR II Station in autumn (October) was around 500 m (Sinclair et al., 2022),
 566 explaining why we found higher BC concentration at high altitudes. For comparison, Table 3 shows the BC
 567 mass concentrations measured at high altitudes in different areas.

568 Table 3. Average BC concentrations observed at different locations.

Location	Altitude	Environment	Average BC concentration (ng m ⁻³)	Reference
Hyytiälä, Finland	100 m	Boreal forest	2278±1188	This study
Hyytiälä, Finland	200 m	Boreal forest	2500±1497	This study
Hyytiälä, Finland	300 m	Boreal forest	3564±1648	This study
Hyytiälä, Finland	400 m	Boreal forest	3909±729	This study
Hyytiälä, Finland	4 m	Boreal forest	320 – 1291 ± 337*	(Hyvärinen et al., 2011)
Mahabaleswar, India	1378 m	Rural	2600 ± 260	(Meena et al., 2021)
Mountain Huang, China	1840 m	Rural	1663±919	(Pan et al., 2011)
Port Blair, India	73 m	Rural	2446±66	(Moorthy and Babu, 2006)
Sinhagad, India	1300 m	Rural	1500	(Safai et al., 2007)

569 *320 ng m⁻³ was the annual average, while 1291 ng m⁻³ was the concentration average measured during pollution event in Autumn

570 Autumn average of BC pollution in Hyytiälä according to Hyvärinen *et al.* 2011 was about 1291 ng m⁻³,
 571 while Hienola *et al* (2013) reported the October average was 550 ng m⁻³ (Hyvärinen et al., 2011; Hienola et
 572 al., 2013). However, those studies were conducted using reference instrument at low altitude, i.e. 4 meters
 573 above the ground.



574

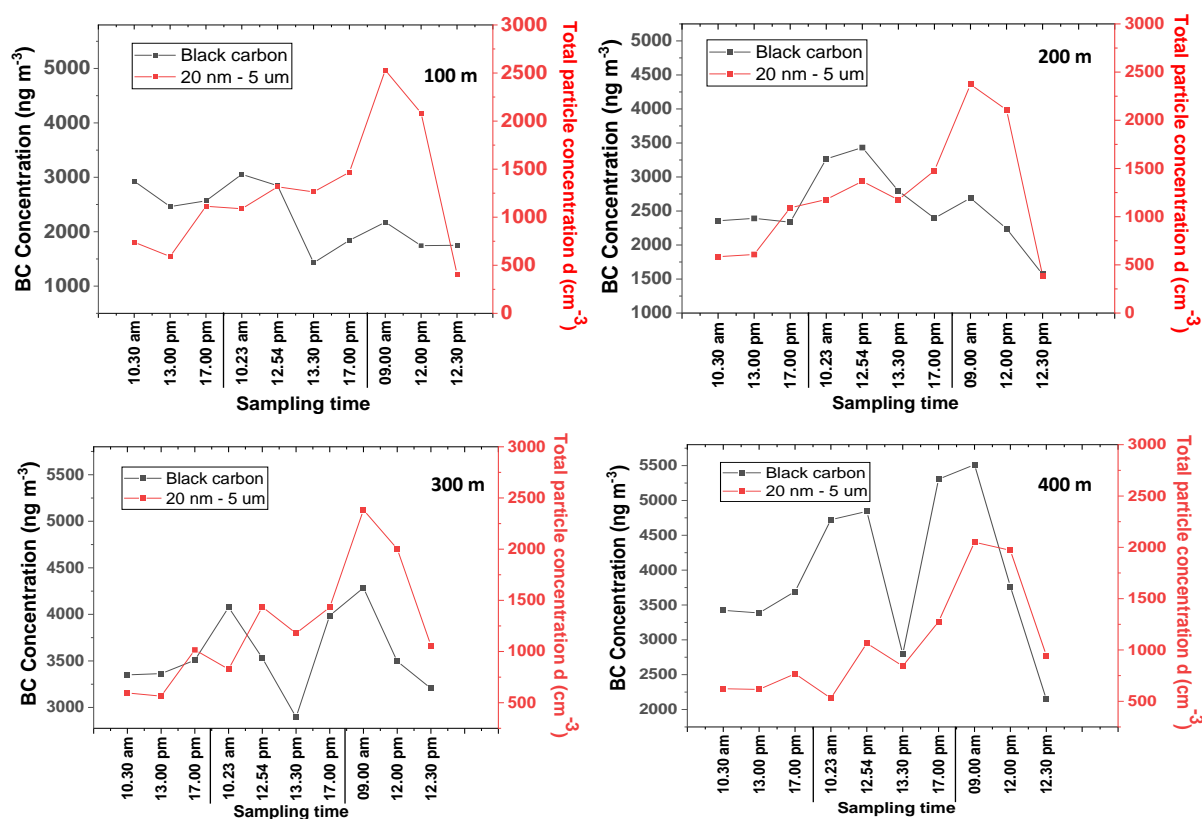
575 **Figure 6.** Evaluation of drone's vertical and horizontal movements. I = Drone is moving up with the speed
576 of 2.5 ms^{-1} . II= Drone is descending with the speed of 1.25 ms^{-1} to each altitude before staying for 30 s. III
577 and IV = Horizontal movement to 100 m far with the speed of 5 ms^{-1} .

578 The drone stability was evaluated during the vertical and horizontal movements (drone movement schematic
579 is showed in Supplemental Fig. S4). Figure 6 shows that the BC concentration and total particle numbers
580 were affected by the drone movements. Rapid ascending (area number I) affected both BC and CPC. BC
581 measurements showed negative values when the drone started warming up, take off, and then quickly moved
582 vertically with the speed of 2.5 ms^{-1} . These readings could be due to the temperature change on the BC sensor
583 when the drone ready to take off and drone fast ascending (Pan et al., 2011; Elomaa, 2022). Portable CPC
584 device gave also fluctuating data. Both BC device and CPC started to stabilize when approaching altitude of
585 365 m.

586 At the beginning of drone vertical movement at the altitude of 400 m, portable CPC gave more stable results
587 when the speed was decreased and when it was allowed to stabilize for 30 seconds (as can be seen in area
588 number II), resulting in smooth changes in the total particle numbers and some deviations at each altitude.
589 However, BC concentration varied also with high standard deviations at high altitude without any specific
590 movement, indicating that the drone movement influenced the portable BC device. Pan *et al* (2011) have
591 suggested that a large variation in the BC measurements could be caused by several factors such as boundary
592 layer stratification and turbulence. In addition, BC sensor was also very sensitive to change in temperature.
593 They observed that BC concentration could change quickly only after a short period of sunshine. Based on

594 the standard deviations' horizontal movements (area numbers III and IV), affected much less portable CPC,
 595 compared to the portable BC.

596



597 **Figure 7.** Time series evaluation of CPC and black carbon at the heights of 100, 200, 300, and 400 m.
 598 Sampling was conducted on October 9 (Day 1), 10 (Day 2), and 11 (Day 3), 2021. The values and point
 599 averages are shown in Supplemental Table S11.

600 It can be seen from the results of Fig. 7 for three days measurements that BC and CPC had similar pattern at
 601 all altitudes (100, 200, 300 and 400 m). The daily means of total particle numbers are found from
 602 Supplemental Table S12. Although the concentrations at the altitude of 400 m seem to be slightly lower than
 603 those detected at lower altitudes, the patterns of total particle number are similar at every altitude (Fig. 7),
 604 most possible due to the limited anthropogenic activities near the sampling site. The potential mixing and the
 605 particle formation in the atmosphere most likely influenced the total particle number detected. In addition,
 606 particulates' long-range transport from different areas could also affect the total particle concentration in the
 607 air (Casquero-Vera et al., 2020).

608 Figure 7 also demonstrates that diurnal pattern was different, revealing that the particle concentrations at
 609 different times of the day were influenced by different sources compared to BC. Almost at all altitudes, the

610 diurnal variation for day 1 and day 2 included a late afternoon peak at 17:00. The particle concentrations
611 increased significantly on the day 3, especially during the first and second samplings before the change to
612 lower concentrations. The samplings for the first two days were carried out during the weekend without many
613 activities that produce VOCs, opposite to Monday morning, when the normal working activities close to
614 sampling area were going-on.

615 In contrast to the pattern of total particle numbers, the daily average of BC concentration during the
616 measurement time period was increased at higher altitudes (Supplemental Table S12), indicating that BC
617 pollutant was distributed from different areas. These trends agree well with the earlier studies (Tripathi et al.,
618 2007). Figure 7 shows that BC diurnal pattern was similar with that of total particle numbers, except on day
619 2 when BC concentration decreased significantly at 13.30, excluding the altitude of 200 m. However, BC
620 concentration increased again at 17.00 most likely due to e.g. sauna heating and air mixing following long-
621 range transport from different areas.

622 During the measurement time, BC at high altitudes 400 m and total particle numbers at all altitudes (100 –
623 400 m) showed diurnal cycle with peak observed on Monday morning at 09:00 am, possible due to morning
624 traffic, and/or to wind-driven pollution transport as suggested by previous studies (Bonasoni et al., 2010;
625 Sandeep et al., 2022). The high BC concentration at high altitude, especially at 400 m, was mostly caused by
626 long-range transport and the atmospheric boundary layer height as discussed earlier, and BC and also other
627 particles contributed to the total particle numbers.

628 **4. Conclusions**

629 An aerial drone carrying the reliable and versatile miniaturized air sampling systems SPME Arrow and ITEX
630 and portable BC and CPC devices was successfully used for the collection of air samples. Up to 48 VOCs
631 were detected in gas and particle phase samples, and their distribution at the altitude from 50 to 400 m was
632 studied. Some differences between VOC compositions at the altitude 50 and 400 m could be explained by
633 the different sources of the VOC emissions. The compounds that most probably originate from the same
634 source had a linear correlation, as well as the compounds that were present both in gas and particle phase
635 samples. The capability of ITEX sampler, furnished with filter accessory for the collection of gas phase
636 samples, was evaluated by comparing it with SPME Arrow sampling resulting in high agreement especially
637 for polar compounds with recoveries up to 99 %. In contrast, non-polar compounds gave low recoveries due
638 to the *like dissolve like* rule meaning that non-polar compounds might be adsorbed to the non-polar PTFE
639 filter of the ITEX sampling system.

640 The portable CPC gave comparable results with those obtained by the conventional reference CPC
641 instruments at the SMEAR II Station, opposite to the portable BC device that was affected by drone's vertical
642 and horizontal movements. The total particle number and BC gave similar diurnal pattern, indicating that
643 they were correlated. The pattern was observed during the weekend. The highest concentrations were found
644 during times with human activities. The distribution was also similar to VOCs that were produced by
645 anthropogenic sources and found in high altitude samples, since the wind most probably carried the VOCs
646 from other sites. For spatial distribution pattern, BC concentrations were increased at higher altitudes due to
647 long-range transport and the atmospheric boundary layer height. The total particle numbers, affected by the
648 similar factors, varied more depending on the sources. This can be explained by the different VOCs that
649 contributed to the particle formations, and the particle sizes measured by the portable CPC and BC monitors.

650 Overall, our study work described a drone equipped with miniaturized air sampling techniques, SPME Arrow
651 and ITEX together with portable BC and CPC devices were for the collection of atmospheric VOCs and for
652 the measurement of BC and total number of particles at high altitudes. To further improve the reliability of
653 the results in the future, a portable BC monitor that includes a better electronic model and the possibility to
654 adjust the device position in the drone are needed.

655 **Author contributions.** EDP, JR-J, JH, KH, MJ, TP and M-LR designed the experiments. EDP, AT, MS, JR-
656 J carried out the experiments. EDP performed data interpretation and visualization. JR-J performed the
657 statistical analysis. YW, JH, JK and KL were responsible for CPC and BC hardware, software and reference
658 data. EDP, JR-J, KH, TP and M-LR prepared the manuscript with contributions from other co-authors.

659

660 **Declaration of competing Interest.** One of the (co-)authors is a member of the editorial board of
661 *Atmospheric Chemistry and Physics*. The peer-review process was guided by an independent editor, and the
662 authors have also no other competing interests to declare.

663 **Acknowledgments.** Financial support was provided by the Jane and Aatos Erkkö Foundation and Academy
664 of Finland (ACCC flagship "Finnish Research Flagship" grant no. 337549). CTC Analytics AG (Zwingen,
665 Switzerland) and BGB Analytik AG (Zürich, Switzerland) are thanked for the cooperation. Tapio Elomaa is
666 also acknowledged for the fruitful discussion especially about Black Carbon (BC) and Condensation Particle
667 Counters (CPCs). In addition, we also thank the staff of the SMEAR II Station, Hyytiälä, for the valuable
668 help.

669 **References**

- 670 Ahlberg, E., Falk, J., Eriksson, A., Holst, T., Brune, W. H., Kristensson, A., Roldin, P., and Svenningsson, B.:
671 Secondary organic aerosol from VOC mixtures in an oxidation flow reactor, *Atmos. Environ.*, 161, 210–220,
672 <https://doi.org/10.1016/j.atmosenv.2017.05.005>, 2017.
- 673 Almeida, J., Schobesberger, S., Kürten, A., Ortega, I. K., Kupiainen-Määttä, O., Praplan, A. P., Adamov, A.,
674 Amorim, A., Bianchi, F., Breitenlechner, M., David, A., Dommen, J., Donahue, N. M., Downard, A., Dunne, E.,
675 Duplissy, J., Ehrhart, S., Flagan, R. C., Franchin, A., Guida, R., Hakala, J., Hansel, A., Heinritzi, M., Henschel, H.,
676 Jokinen, T., Junninen, H., Kajos, M., Kangasluoma, J., Keskinen, H., Kupc, A., Kurtén, T., Kvashin, A. N.,
677 Laaksonen, A., Lehtipalo, K., Leiminger, M., Leppä, J., Loukonen, V., Makhmutov, V., Mathot, S., McGrath, M. J.,
678 Nieminen, T., Olenius, T., Onnela, A., Petäjä, T., Riccobono, F., Riipinen, I., Rissanen, M., Rondo, L., Ruuskanen,
679 T., Santos, F. D., Sarnela, N., Schallhart, S., Schnitzhofer, R., Seinfeld, J. H., Simon, M., Sipilä, M., Stozhkov, Y.,
680 Stratmann, F., Tomé, A., Tröstl, J., Tsagkogeorgas, G., Vaattovaara, P., Viisanen, Y., Virtanen, A., Vrtala, A.,
681 Wagner, P. E., Weingartner, E., Wex, H., Williamson, C., Wimmer, D., Ye, P., Yli-Juuti, T., Carslaw, K. S.,
682 Kulmala, M., Curtius, J., Baltensperger, U., Worsnop, D. R., Vehkamäki, H., and Kirkby, J.: Molecular
683 understanding of sulphuric acid-amine particle nucleation in the atmosphere, *Nature*, 502, 359–363,
684 <https://doi.org/10.1038/nature12663>, 2013.
- 685 Altshuller, A. P.: Production of aldehydes as primary emissions and from secondary atmospheric reactions of alkenes
686 and alkanes during the night and early morning hours, *Atmos. Environ. Part A, Gen. Top.*, 27, 21–32,
687 [https://doi.org/10.1016/0960-1686\(93\)90067-9](https://doi.org/10.1016/0960-1686(93)90067-9), 1993.
- 688 Anenberg, S. C., Schwartz, J., Shindell, D., Amann, M., Faluvegi, G., Klimont, Z., Janssens-Maenhout, G., Pozzoli,
689 L., van Dingenen, R., Vignati, E., Emberson, L., Muller, N. Z., Jason West, J., Williams, M., Demkine, V., Kevin
690 Hicks, W., Kuylenstierna, J., Raes, F., and Ramanathan, V.: Global air quality and health co-benefits of mitigating
691 near-term climate change through methane and black carbon emission controls, *Environ. Health Perspect.*, 120, 831–
692 839, <https://doi.org/10.1289/ehp.1104301>, 2012.
- 693 Asbach, C., Schmitz, A., Schmidt, F., Monz, C., and Todea, A. M.: Intercomparison of a personal CPC and different
694 conventional CPCs, *Aerosol Air Qual. Res.*, 17, 1132–1141, <https://doi.org/10.4209/aaqr.2016.10.0460>, 2017.
- 695 Bonasoni, P., Laj, P., Marinoni, A., Sprenger, M., Angelini, F., Arduini, J., Bonafè, U., Calzolari, F., Colombo, T.,
696 Decesari, S., Di Biagio, C., Di Sarra, A. G., Evangelisti, F., Duchi, R., Facchini, M. C., Fuzzi, S., Gobbi, G. P.,
697 Maione, M., Panday, A., Roccatò, F., Sellegri, K., Venzac, H., Verza, G. P., Villani, P., Vuillermoz, E., and
698 Cristofanelli, P.: Atmospheric Brown Clouds in the Himalayas: First two years of continuous observations at the
699 Nepal Climate Observatory-Pyramid (5079 m), *Atmos. Chem. Phys.*, 10, 7515–7531, <https://doi.org/10.5194/acp-10-7515-2010>, 2010.
- 701 Bonn, B., von Kuhlmann, R., and Lawrence, M. G.: High contribution of biogenic hydroperoxides to secondary
702 organic aerosol formation, *Geophys. Res. Lett.*, 31, 1–4, <https://doi.org/10.1029/2003GL019172>, 2004.
- 703 Boylstein, R., Piacitelli, C., Grote, A., Kanwal, R., Kullman, G., and Kreiss, K.: Diacetyl emissions and airborne dust
704 from butter flavorings used in microwave popcorn production, *J. Occup. Environ. Hyg.*, 3, 530–535,
705 <https://doi.org/10.1080/15459620600909708>, 2006.
- 706 Brasseur, G. P., Orlando, J. J., and Tyndall, G. S.: *Atmospheric Chemistry and Global Change*, Oxford University
707 Press, New York, 1999.
- 708 Buzorius, G., Rannik, Ü., Mäkelä, J. M., Vesala, T., and Kulmala, M.: Vertical aerosol particle fluxes measured by
709 eddy covariance technique using condensational particle counter, *J. Aerosol Sci.*, 29, 157–171,
710 [https://doi.org/10.1016/S0021-8502\(97\)00458-8](https://doi.org/10.1016/S0021-8502(97)00458-8), 1998.
- 711 Camredon, M., Aumont, B., Lee-Taylor, J., and Madronich, S.: The SOA/VOC/NO_x system: an explicit model of
712 secondary organic aerosol formation, *Atmos. Chem. Phys.*, 5599–5610 pp., 2007.
- 713 Carnerero, C., Pérez, N., Reche, C., Ealo, M., Titos, G., Lee, H. K., Eun, H. R., Park, Y. H., Dada, L., Paasonen, P.,
714 Kerminen, V. M., Mantilla, E., Escudero, M., Gómez-Moreno, F. J., Alonso-Blanco, E., Coz, E., Saiz-Lopez, A.,
715 Temime-Roussel, B., Marchand, N., Beddows, D. C. S., Harrison, R. M., Petäjä, T., Kulmala, M., Ahn, K. H.,
716 Alastuey, A., and Querol, X.: Vertical and horizontal distribution of regional new particle formation events in

- 717 Madrid, *Atmos. Chem. Phys.*, 18, 16601–16618, <https://doi.org/10.5194/acp-18-16601-2018>, 2018.
- 718 Casquero-Vera, J. A., Lyamani, H., Dada, L., Hakala, S., Paasonen, P., Román, R., Fraile, R., Petäjä, T., Olmo-
719 Reyes, F. J., and Alados-Arboledas, L.: New particle formation at urban and high-altitude remote sites in the south-
720 eastern Iberian Peninsula, *Atmos. Chem. Phys.*, 20, 14253–14271, <https://doi.org/10.5194/acp-20-14253-2020>, 2020.
- 721 Chen, J., Jiang, S., Liu, Y. R., Huang, T., Wang, C. Y., Miao, S. K., Wang, Z. Q., Zhang, Y., and Huang, W.:
722 Interaction of oxalic acid with dimethylamine and its atmospheric implications, *RSC Adv.*, 7, 6374–6388,
723 <https://doi.org/10.1039/c6ra27945g>, 2017.
- 724 Chen, J., Scircle, A., Black, O., Cizdziel, J. V., Watson, N., Wevill, D., and Zhou, Y.: On the use of multicopters for
725 sampling and analysis of volatile organic compounds in the air by adsorption/thermal desorption GC-MS, *Air Qual.*
726 *Atmos. Heal.*, 11, 835–842, <https://doi.org/10.1007/s11869-018-0588-y>, 2018.
- 727 Chen, T., Ge, Y., Liu, Y., and He, H.: N-nitration of secondary aliphatic amines in the particle phase, *Chemosphere*,
728 293, 133639, <https://doi.org/10.1016/j.chemosphere.2022.133639>, 2022.
- 729 Correa, S. M., Arbilla, G., Marques, M. R. C., and Oliveira, K. M. P. G.: The impact of BTEX emissions from gas
730 stations into the atmosphere, *Atmos. Pollut. Res.*, 3, 163–169, <https://doi.org/10.5094/APR.2012.016>, 2012.
- 731 Dehghani, M., Fazlzadeh, M., Sorooshian, A., Tabatabaee, H. R., Miri, M., Baghani, A. N., Delikhoon, M., Mahvi,
732 A. H., and Rashidi, M.: Characteristics and health effects of BTEX in a hot spot for urban pollution, *Ecotoxicol.*
733 *Environ. Saf.*, 155, 133–143, <https://doi.org/10.1016/j.ecoenv.2018.02.065>, 2018.
- 734 Dou, J., Lin, P., Kuang, B. Y., and Yu, J. Z.: Reactive oxygen species production mediated by humic-like substances
735 in atmospheric aerosols: Enhancement effects by pyridine, imidazole, and their derivatives, *Environ. Sci. Technol.*,
736 49, 6457–6465, <https://doi.org/10.1021/es5059378>, 2015.
- 737 Dumka, U. C., Moorthy, K. K., Kumar, R., Hegde, P., Sagar, R., Pant, P., Singh, N., and Babu, S. S.: Characteristics
738 of aerosol black carbon mass concentration over a high altitude location in the Central Himalayas from multi-year
739 measurements, *Atmos. Res.*, 96, 510–521, <https://doi.org/10.1016/j.atmosres.2009.12.010>, 2010.
- 740 Elomaa, T.: *Mustan hiilen mittausta suodatinpohjaisilla sensoreilla*, University of Helsinki, 2022.
- 741 Fermo, P., Artñano, B., De Gennaro, G., Pantaleo, A. M., Parente, A., Battaglia, F., Colicino, E., Di Tanna, G.,
742 Goncalves da Silva Junior, A., Pereira, I. G., Garcia, G. S., Garcia Goncalves, L. M., Comite, V., and Miani, A.:
743 Improving indoor air quality through an air purifier able to reduce aerosol particulate matter (PM) and volatile
744 organic compounds (VOCs): Experimental results, *Environ. Res.*, 197, 1–8,
745 <https://doi.org/10.1016/j.envres.2021.111131>, 2021.
- 746 Fu, P., Kawamura, K., Usukura, K., and Miura, K.: Dicarboxylic acids, ketocarboxylic acids and glyoxal in the
747 marine aerosols collected during a round-the-world cruise, *Mar. Chem.*, 148, 22–32,
748 <https://doi.org/10.1016/j.marchem.2012.11.002>, 2013.
- 749 Ge, X., Wexler, A. S., and Clegg, S. L.: Atmospheric amines - Part I. A review, *Atmos. Environ.*, 45, 524–546,
750 <https://doi.org/10.1016/j.atmosenv.2010.10.012>, 2011.
- 751 De Haan, D. O., Hawkins, L. N., Kononenko, J. A., Turley, J. J., Corrigan, A. L., Tolbert, M. A., and Jimenez, J. L.:
752 Formation of nitrogen-containing oligomers by methylglyoxal and amines in simulated evaporating cloud droplets,
753 *Environ. Sci. Technol.*, 45, 984–991, <https://doi.org/10.1021/es102933x>, 2011.
- 754 Hari, P. and Kulmala, M.: Station for Measuring Ecosystem-Atmosphere Relations (SMEAR II), *Boreal Environ.*
755 *Res.*, 10, 315–322, 2005.
- 756 Helin, A., Rönkkö, T., Parshintsev, J., Hartonen, K., Schilling, B., Läubli, T., and Riekkola, M. L.: Solid phase
757 microextraction Arrow for the sampling of volatile amines in wastewater and atmosphere, *J. Chromatogr. A*, 1426,
758 56–63, <https://doi.org/10.1016/j.chroma.2015.11.061>, 2015.
- 759 Hemmilä, M.: *Chemical Characterisation of Boreal Forest Air with Chromatographic Techniques*, University of
760 Helsinki, Helsinki, 2020.

- 761 Hemmilä, M., Hellén, H., Virkkula, A., Makkonen, U., Praplan, A. P., Kontkanen, J., Ahonen, L., Kulmala, M., and
762 Hakola, H.: Amines in boreal forest air at SMEAR II station in Finland, *Atmos. Chem. Phys.*, 18, 6367–6380,
763 <https://doi.org/10.5194/acp-18-6367-2018>, 2018.
- 764 Hienola, A. I., Pietikäinen, J. P., Jacob, D., Pozdun, R., Petäjä, T., Hyvärinen, A. P., Sogacheva, L., Kerminen, V.
765 M., Kulmala, M., and Laaksonen, A.: Black carbon concentration and deposition estimations in Finland by the
766 regional aerosol-climate model REMO-HAM, *Atmos. Chem. Phys.*, 13, 4033–4055, <https://doi.org/10.5194/acp-13-4033-2013>, 2013.
- 768 Hoeben, W. F. L. M., Beckers, F. J. C. M., Pemen, A. J. M., Van Heesch, E. J. M., and Kling, W. L.: Oxidative
769 degradation of toluene and limonene in air by pulsed corona technology, *J. Phys. D. Appl. Phys.*, 45,
770 <https://doi.org/10.1088/0022-3727/45/5/055202>, 2012.
- 771 Hyvärinen, A. P., Kolmonen, P., Kerminen, V. M., Virkkula, A., Leskinen, A., Komppula, M., Hatakka, J., Burkhart,
772 J., Stohl, A., Aalto, P., Kulmala, M., Lehtinen, K. E. J., Viisanen, Y., and Lihavainen, H.: Aerosol black carbon at
773 five background measurement sites over Finland, a gateway to the Arctic, *Atmos. Environ.*, 45, 4042–4050,
774 <https://doi.org/10.1016/j.atmosenv.2011.04.026>, 2011.
- 775 Isidorov, V. A., Pirožnikow, E., Spirina, V. L., Vasyanin, A. N., Kulakova, S. A., Abdulmanova, I. F., and Zaitsev,
776 A. A.: Emission of volatile organic compounds by plants on the floor of boreal and mid-latitude forests, *J. Atmos.
777 Chem.*, 79, 153–166, <https://doi.org/10.1007/s10874-022-09434-3>, 2022.
- 778 Jacobson, M. Z.: Short-term effects of controlling fossil-fuel soot, biofuel soot and gases, and methane on climate,
779 Arctic ice, and air pollution health, *J. Geophys. Res. Atmos.*, 115, <https://doi.org/10.1029/2009JD013795>, 2010.
- 780 Jang, M. and Kamens, R. M.: Atmospheric secondary aerosol formation by heterogeneous reactions of aldehydes in
781 the presence of a sulfuric acid aerosol catalyst, *Environ. Sci. Technol.*, 35, 4758–4766,
782 <https://doi.org/10.1021/es010790s>, 2001.
- 783 Junninen, H., Lauri, A., Keronen, P., Aalto, P., Hiltunen, V., Hari, P., and Kulmala, M.: Smart-SMEAR: On-line data
784 exploration and visualization tool for SMEAR stations, *Boreal Environ. Res.*, 14, 447–457, 2009.
- 785 Kamens, R. M., Zhang, H., Chen, E. H., Zhou, Y., Parikh, H. M., Wilson, R. L., Galloway, K. E., and Rosen, E. P.:
786 Secondary organic aerosol formation from toluene in an atmospheric hydrocarbon mixture: Water and particle seed
787 effects, *Atmos. Environ.*, 45, 2324–2334, <https://doi.org/10.1016/j.atmosenv.2010.11.007>, 2011.
- 788 Kanakidou, M., Seinfeld, J. H., Pandis, S. N., Barnes, I., Dentener, F. J., Facchini, M. C., Van Dingenen, R., Ervens,
789 B., Nenes, A., Nielsen, C. J., Swietlicki, E., Putaud, J. P., Balkanski, Y., Fuzzi, S., Horth, J., Moortgat, G. K.,
790 Winterhalter, R., Myhre, C. E. L., Tsigaridis, K., Vignati, E., Stephanou, E. G., and Wilson, J.: Organic aerosol and
791 global climate modelling: A review, *Atmos. Chem. Phys.*, 5, 1053–1123, <https://doi.org/10.5194/acp-5-1053-2005>,
792 2005.
- 793 Kangasluoma, J. and Attoui, M.: Review of sub-3 nm condensation particle counters, calibrations, and cluster
794 generation methods, *Aerosol Sci. Technol.*, 53, 1277–1310, <https://doi.org/10.1080/02786826.2019.1654084>, 2019.
- 795 Karlberg, A. -T, Magnusson, K., and Nilsson, U.: Air oxidation of d-limonene (the citrus solvent) creates potent
796 allergens, *Contact Dermatitis*, 26, 332–340, <https://doi.org/10.1111/j.1600-0536.1992.tb00129.x>, 1992.
- 797 Kawamura, K. and Sakaguchi, F.: Acids Were Detected in the Sample3S). With a Concentration Range of, North,
798 104, 3501–3509, 1999.
- 799 Khare, P., Kumar, N., Kumari, K. M., and Srivastava, S. S.: Atmospheric formic acid and acetic acids : an overview,
800 *Rev. Geophys.*, 227–248, 1999.
- 801 Kieloaho, A.: Alkyl Amines in Boreal Forest and Urban Area, 2017.
- 802 Kim, H., Park, Y., Kim, W., and Eun, H.: Vertical Aerosol Distribution and Flux Measurement in the Planetary
803 Boundary Layer Using Drone, 14, 35–40, 2018.
- 804 Kim, S. H., Kirakosyan, A., Choi, J., and Kim, J. H.: Detection of volatile organic compounds (VOCs), aliphatic

805 amines, using highly fluorescent organic-inorganic hybrid perovskite nanoparticles, *Dye. Pigment.*, 147, 1–5,
806 <https://doi.org/10.1016/j.dyepig.2017.07.066>, 2017.

807 Kim, S. J., Lee, J. Y., Choi, Y. S., Sung, J. M., and Jang, H. W.: Comparison of different types of SPME arrow
808 sorbents to analyze volatile compounds in *cirsium setidens nakai*, *Foods*, 9, <https://doi.org/10.3390/foods9060785>,
809 2020.

810 Kivekäs, N., Sun, J., Zhan, M., Kerminen, V., Hyvärinen, A., Komppula, M., Viisanen, Y., Hong, N., Zhang, Y.,
811 Kulmala, M., Zhang, X., and Lihavainen, H.: Long term particle size distribution measurements at Mount Waliguan,
812 a high-altitude site in inland China, *Atmos. Chem. Phys.*, 5461–5474 pp., 2009.

813 Kopperi, M., Ruiz-Jiménez, J., Hukkinen, J. I., and Riekkola, M. L.: New way to quantify multiple steroidal
814 compounds in wastewater by comprehensive two-dimensional gas chromatography-time-of-flight mass spectrometry,
815 *Anal. Chim. Acta*, 761, 217–226, <https://doi.org/10.1016/j.aca.2012.11.059>, 2013.

816 Kristensen, K., Bilde, M., Aalto, P. P., Petäjä, T., and Glasius, M.: Denuder/filter sampling of organic acids and
817 organosulfates at urban and boreal forest sites: Gas/particle distribution and possible sampling artifacts, *Atmos.*
818 *Environ.*, 130, 36–53, <https://doi.org/10.1016/j.atmosenv.2015.10.046>, 2016.

819 Krue, A.: Influence of mobile phase, source parameters and source type on electrospray ionization efficiency in
820 negative ion mode, *J. Mass Spectrom.*, 51, 596–601, <https://doi.org/10.1002/jms.3790>, 2016.

821 Kulmala, M., Kontkanen, J., Junninen, H., Lehtipalo, K., Manninen, H. E., Nieminen, T., Petäjä, T., Sipilä, M.,
822 Schobesberger, S., Rantala, P., Franchin, A., Jokinen, T., Järvinen, E., Äijälä, M., Kangasluoma, J., Hakala, J., Aalto,
823 P. P., Paasonen, P., Mikkilä, J., Vanhanen, J., Aalto, J., Hakola, H., Makkonen, U., Ruuskanen, T., Mauldin, R. L.,
824 Duplissy, J., Vehkamäki, H., Bäck, J., Kortelainen, A., Riipinen, I., Kurtén, T., Johnston, M. V., Smith, J. N., Ehn,
825 M., Mentel, T. F., Lehtinen, K. E. J., Laaksonen, A., Kerminen, V. M., and Worsnop, D. R.: Direct observations of
826 atmospheric aerosol nucleation, *Science* (80-.), 339, 943–946, <https://doi.org/10.1126/science.1227385>, 2013.

827 Kulmala, M., Petäjä, T., Ehn, M., Thornton, J., Sipilä, M., Worsnop, D. R., and Kerminen, V. M.: Chemistry of
828 atmospheric nucleation: On the recent advances on precursor characterization and atmospheric cluster composition in
829 connection with atmospheric new particle formation, *Annu. Rev. Phys. Chem.*, 65, 21–37,
830 <https://doi.org/10.1146/annurev-physchem-040412-110014>, 2014.

831 Kumar, R., Barth, M. C., Nair, V. S., Pfister, G. G., Suresh Babu, S., Satheesh, S. K., Krishna Moorthy, K.,
832 Carmichael, G. R., Lu, Z., and Streets, D. G.: Sources of black carbon aerosols in South Asia and surrounding
833 regions during the Integrated Campaign for Aerosols, Gases and Radiation Budget (ICARB), *Atmos. Chem. Phys.*,
834 15, 5415–5428, <https://doi.org/10.5194/acp-15-5415-2015>, 2015.

835 Lan, H., Holopainen, J., Hartonen, K., Jussila, M., Ritala, M., and Riekkola, M. L.: Fully Automated Online
836 Dynamic In-Tube Extraction for Continuous Sampling of Volatile Organic Compounds in Air, *Anal. Chem.*, 91,
837 8507–8515, <https://doi.org/10.1021/acs.analchem.9b01668>, 2019a.

838 Lan, H., Zhang, W., Smått, J.-H., Koivula, R. T., Hartonen, K., and Riekkola, M.-L.: Selective extraction of aliphatic
839 amines by functionalized mesoporous silica-coated solid phase microextraction Arrow, *Microchim. Acta*, 186, 412,
840 <https://doi.org/10.1007/s00604-019-3523-5>, 2019b.

841 Lan, H., Hartonen, K., and Riekkola, M. L.: Miniaturised air sampling techniques for analysis of volatile organic
842 compounds in air, *TrAC - Trends Anal. Chem.*, 126, 115873, <https://doi.org/10.1016/j.trac.2020.115873>, 2020.

843 Lan, H., Ruiz-Jimenez, J., Leleev, Y., Demaria, G., Jussila, M., Hartonen, K., and Riekkola, M.-L.: Quantitative
844 analysis and spatial and temporal distribution of volatile organic compounds in atmospheric air by utilizing drone
845 with miniaturized samplers, *Chemosphere*, 282, 131024, <https://doi.org/10.1016/j.chemosphere.2021.131024>, 2021.

846 Liu, Y., Monod, A., Tritscher, T., Praplan, A. P., Decarlo, P. F., Temime-Roussel, B., Quivet, E., Marchand, N.,
847 Dommen, J., and Baltensperger, U.: Aqueous phase processing of secondary organic aerosol from isoprene
848 photooxidation, *Atmos. Chem. Phys.*, 12, 5879–5895, <https://doi.org/10.5194/acp-12-5879-2012>, 2012.

849 McGillen, M. R., Curchod, B. F. E., Chhantyal-Pun, R., Beames, J. M., Watson, N., Khan, M. A. H., McMahon, L.,

850 Shallcross, D. E., and Orr-Ewing, A. J.: Criegee Intermediate-Alcohol Reactions, A Potential Source of
851 Functionalized Hydroperoxides in the Atmosphere, *ACS Earth Sp. Chem.*, 1, 664–672,
852 <https://doi.org/10.1021/acsearthspacechem.7b00108>, 2017.

853 McMurry, P. H.: The history of condensation nucleus counters, *Aerosol Sci. Technol.*, 33, 297–322,
854 <https://doi.org/10.1080/02786820050121512>, 2000.

855 Meena, G. S., Mukherjee, S., Buchunde, P., Safai, P. D., Singla, V., Aslam, M. Y., Sonbawne, S. M., Made, R.,
856 Anand, V., Dani, K. K., and Pandithurai, G.: Seasonal variability and source apportionment of black carbon over a
857 rural high-altitude and an urban site in western India, *Atmos. Pollut. Res.*, 12, 32–45,
858 <https://doi.org/10.1016/j.apr.2020.10.006>, 2021.

859 Moorthy, K. K. and Babu, S. S.: Aerosol black carbon over Bay of Bengal observed from an island location, Port
860 Blair: Temporal features and long-range transport, *J. Geophys. Res. Atmos.*, 111, 1–10,
861 <https://doi.org/10.1029/2005JD006855>, 2006.

862 Ng, N. L., Kroll, J. H., Chan, A. W. H., Chhabra, P. S., Flagan, R., and Seinfeld, J. H.: Pytannia Vzaiemodii
863 Partyzaniv Z Chastynamy Chervonoi Armii Pid Chas Vyzvolennia Pravoberezhnoi Ukrainy V Radians’Kii
864 Istoriohrafii., *Atmos. Chem. Phys.*, 7, 3909–3922, 2007.

865 Nguyen, H. T. H., Takenaka, N., Bandow, H., Maeda, Y., De Oliva, S. T., Botelho, M. M. F., and Tavares, T. M.:
866 Atmospheric alcohols and aldehydes concentrations measured in Osaka, Japan and in Sao Paulo, Brazil, *Atmos.*
867 *Environ.*, 35, 3075–3083, [https://doi.org/10.1016/S1352-2310\(01\)00136-4](https://doi.org/10.1016/S1352-2310(01)00136-4), 2001.

868 Oh, H. J., Ma, Y., and Kim, J.: Human inhalation exposure to aerosol and health effect: Aerosol monitoring and
869 modelling regional deposited doses, *Int. J. Environ. Res. Public Health*, 17, 1–2,
870 <https://doi.org/10.3390/ijerph17061923>, 2020.

871 Olsen, R., Thorud, S., Heresson, M., Øvrebø, S., Lundanes, E., Greibrokk, T., Ellingsen, D. G., Thomassen, Y., and
872 Molander, P.: Determination of the dialdehyde glyoxal in workroom air - Development of personal sampling
873 methodology, *J. Environ. Monit.*, 9, 687–694, <https://doi.org/10.1039/b700105n>, 2007.

874 Pan, X. L., Kanaya, Y., Wang, Z. F., Liu, Y., Pochanart, P., Akimoto, H., Sun, Y. L., Dong, H. B., Li, J., Irie, H., and
875 Takigawa, M.: Correlation of black carbon aerosol and carbon monoxide in the high-altitude environment of Mt.
876 Huang in Eastern China, *Atmos. Chem. Phys.*, 11, 9735–9747, <https://doi.org/10.5194/acp-11-9735-2011>, 2011.

877 Parshintsev, J., Ruiz-Jimenez, J., Petäjä, T., Hartonen, K., Kulmala, M., and Riekkola, M. L.: Comparison of quartz
878 and Teflon filters for simultaneous collection of size-separated ultrafine aerosol particles and gas-phase zero samples,
879 *Anal. Bioanal. Chem.*, 400, 3527–3535, <https://doi.org/10.1007/s00216-011-5041-0>, 2011.

880 Parsons, G. E., Buckton, G., and Chatham B’, S. M.: The use of surface energy and polarity determinations to
881 predict physical stability of non-polar, non-aqueous suspensions, *International Journal of Pharmaceutics*, 163–170
882 pp., 1992.

883 Peng, L., Li, Z., Zhang, G., Bi, X., Hu, W., Tang, M., Wang, X., Peng, P., and Sheng, G.: A review of measurement
884 techniques for aerosol effective density, *Sci. Total Environ.*, 778, 146248,
885 <https://doi.org/10.1016/j.scitotenv.2021.146248>, 2021.

886 Perez, J. E., Kumar, M., Francisco, J. S., and Sinha, A.: Oxygenate-Induced Tuning of Aldehyde-Amine Reactivity
887 and Its Atmospheric Implications, *J. Phys. Chem. A*, 121, 1022–1031, <https://doi.org/10.1021/acs.jpca.6b10845>,
888 2017.

889 Petäjä, T., Rannik, Ü., Buzorius, G., Aalto, P., Vesala, T., and Kulmala, M.: Deposition Velocities of Ultrafine
890 Particles Into Scots Pine Forest During Nucleation Events, *J. Aerosol Sci.*, 32, 143–144,
891 [https://doi.org/10.1016/s0021-8502\(21\)00068-9](https://doi.org/10.1016/s0021-8502(21)00068-9), 2001.

892 Petäjä, T., Laakso, L., Grönholm, T., Launiainen, S., Evele-Peltoniemi, I., Virkkula, A., Leskinen, A., Backman, J.,
893 Manninen, H. E., Sipilä, M., Haapanala, S., Hämeri, K., Vanhala, E., Tuomi, T., Paatero, J., Aurela, M., Hakola, H.,
894 Makkonen, U., Hellén, H., Hillamo, R., Vira, J., Prank, M., Sofiev, M., Siitari-Kauppi, M., Laaksonen, A., lehtinen,

895 K. E. J., Kulmala, M., Viisanen, Y., and Kerminen, V. M.: In-situ observations of Eyjafjallajökull ash particles by
896 hot-air balloon, *Atmos. Environ.*, 48, 104–112, <https://doi.org/10.1016/j.atmosenv.2011.08.046>, 2012.

897 Pusfitasari, E. D., Ruiz-Jimenez, J., Heiskanen, I., Jussila, M., Hartonen, K., and Riekkola, M.-L.: Aerial drone
898 furnished with miniaturized versatile air sampling systems for selective collection of nitrogen containing compounds
899 in boreal forest, *Sci. Total Environ.*, 808, 152011, <https://doi.org/10.1016/J.SCITOTENV.2021.152011>, 2022.

900 Rajesh, T. A. and Ramachandran, S.: Black carbon aerosols over urban and high altitude remote regions:
901 Characteristics and radiative implications, *Atmos. Environ.*, 194, 110–122,
902 <https://doi.org/10.1016/j.atmosenv.2018.09.023>, 2018.

903 Rinaldi, M., Decesari, S., Carbone, C., Finessi, E., Fuzzi, S., Ceburnis, D., O’Dowd, C. D., Sciare, J., Burrows, J. P.,
904 Vrekoussis, M., Ervens, B., Tsigaridis, K., and Facchini, M. C.: Evidence of a natural marine source of oxalic acid
905 and a possible link to glyoxal, *J. Geophys. Res. Atmos.*, 116, 1–12, <https://doi.org/10.1029/2011JD015659>, 2011.

906 Rosado-Reyes, C. M. and Francisco, J. S.: Atmospheric oxidation pathways of acetic acid, *J. Phys. Chem. A*, 110,
907 4419–4433, <https://doi.org/10.1021/jp0567974>, 2006.

908 Ruiz-Jimenez, J., Zanca, N., Lan, H., Jussila, M., Hartonen, K., and Riekkola, M. L.: Aerial drone as a carrier for
909 miniaturized air sampling systems, *J. Chromatogr. A*, 1597, 202–208, <https://doi.org/10.1016/j.chroma.2019.04.009>,
910 2019.

911 Safai, P. D., Kewat, S., Praveen, P. S., Rao, P. S. P., Momin, G. A., Ali, K., and Devara, P. C. S.: Seasonal variation
912 of black carbon aerosols over a tropical urban city of Pune, India, *Atmos. Environ.*, 41, 2699–2709,
913 <https://doi.org/10.1016/j.atmosenv.2006.11.044>, 2007.

914 Sahli, A.: X ; H ; X, 1009–1012, 1992.

915 Sandeep, K., Panicker, A. S., Gautam, A. S., Beig, G., Gandhi, N., S, S., Shankar, R., and Nainwal, H. C.: Black
916 carbon over a high altitude Central Himalayan Glacier: Variability, transport, and radiative impacts, *Environ. Res.*,
917 204, <https://doi.org/10.1016/j.envres.2021.112017>, 2022.

918 Sato, K., Ikemori, F., Ramasamy, S., Fushimi, A., Kumagai, K., Iijima, A., and Morino, Y.: Four- and five-carbon
919 dicarboxylic acids present in secondary organic aerosol produced from anthropogenic and biogenic volatile organic
920 compounds, *Atmosphere (Basel)*, 12, <https://doi.org/10.3390/atmos12121703>, 2021.

921 Sinclair, V. A., Ritvanen, J., Urbancic, G., Statnaia, I., Batrak, Y., Moisseev, D., and Kurppa, M.: Boundary-layer
922 height and surface stability at Hyytiälä, Finland, in ERA5 and observations, *Atmos. Meas. Tech.*, 15, 3075–3103,
923 <https://doi.org/10.5194/amt-15-3075-2022>, 2022.

924 Takahama, S., Schwartz, R. E., Russell, L. M., MacDonald, A. M., Sharma, S., and Leaitch, W. R.: Organic
925 functional groups in aerosol particles from burning and non-burning forest emissions at a high-elevation mountain
926 site, *Atmos. Chem. Phys.*, 11, 6367–6386, <https://doi.org/10.5194/acp-11-6367-2011>, 2011.

927 Teich, M., Schmidpott, M., van Pinxteren, D., Chen, J., and Herrmann, H.: Separation and quantification of
928 imidazoles in atmospheric particles using LC–Orbitrap-MS, *J. Sep. Sci.*, 43, 577–589,
929 <https://doi.org/10.1002/jssc.201900689>, 2020.

930 Tripathi, S. N., Srivastava, A. K., Dey, S., Satheesh, S. K., and Krishnamoorthy, K.: The vertical profile of
931 atmospheric heating rate of black carbon aerosols at Kanpur in northern India, *Atmos. Environ.*, 41, 6909–6915,
932 <https://doi.org/10.1016/j.atmosenv.2007.06.032>, 2007.

933 Weingartner, E., Saathoff, H., Schnaiter, M., Streit, N., Bitnar, B., and Baltensperger, U.: Absorption of light by soot
934 particles: Determination of the absorption coefficient by means of aethalometers, *J. Aerosol Sci.*, 34, 1445–1463,
935 [https://doi.org/10.1016/S0021-8502\(03\)00359-8](https://doi.org/10.1016/S0021-8502(03)00359-8), 2003.

936 Wen, L., Schaefer, T., He, L., Zhang, Y., Sun, X., Ventura, O. N., and Herrmann, H.: T- And pH-Dependent Kinetics
937 of the Reactions of ·OH(aq) with Glutaric and Adipic Acid for Atmospheric Aqueous-Phase Chemistry, *ACS Earth*
938 *Sp. Chem.*, 5, 1854–1864, <https://doi.org/10.1021/acsearthspacechem.1c00163>, 2021.

- 939 Yassaa, N., Brancaleoni, E., Frattoni, M., and Ciccioli, P.: Isomeric analysis of BTEXs in the atmosphere using β -
940 cyclodextrin capillary chromatography coupled with thermal desorption and mass spectrometry, *Chemosphere*, 63,
941 502–508, <https://doi.org/10.1016/j.chemosphere.2005.08.010>, 2006.
- 942 Youn, J.-S., Crosbie, E.S. B., Maudlin, L. C., Wang, Z., and Sorooshian, A.: Dimethylamine as a major alkyl amine
943 species in particles and cloud water: Observations in semi-arid and coastal regions, *Atmos. Environ.*, 122, 250–258,
944 <https://doi.org/doi:10.1016/j.atmosenv.2015.09.061>, 2015.
- 945 Yu, K., Mitch, W. A., and Dai, N.: Nitrosamines and Nitramines in Amine-Based Carbon Dioxide Capture Systems:
946 Fundamentals, Engineering Implications, and Knowledge Gaps, *Environ. Sci. Technol.*, 51, 11522–11536,
947 <https://doi.org/10.1021/acs.est.7b02597>, 2017.
- 948 Zahardis, J., Geddes, S., and Petrucci, G. A.: The ozonolysis of primary aliphatic amines in fine particles, *Atmos.*
949 *Chem. Phys.*, 8, 1181–1194, <https://doi.org/10.5194/acp-8-1181-2008>, 2008.
- 950 Zhang, R., Shen, J., Xie, H.-B., Chen, J., and Elm, J.: The role of organic acids in new particle formation from
951 methanesulfonic acid and methylamine, *Atmos. Chem. Phys.*, 22, 2639–2650, [https://doi.org/doi.org/10.5194/acp-22-](https://doi.org/doi.org/10.5194/acp-22-2639-2022)
952 [2639-2022](https://doi.org/doi.org/10.5194/acp-22-2639-2022), 2022.
- 953 Zhang, Y., Wang, X., Wen, S., Herrmann, H., Yang, W., Huang, X., Zhang, Z., Huang, Z., He, Q., and George, C.:
954 On-road vehicle emissions of glyoxal and methylglyoxal from tunnel tests in urban Guangzhou, China, *Atmos.*
955 *Environ.*, 127, 55–60, <https://doi.org/10.1016/j.atmosenv.2015.12.017>, 2016.
- 956 Zhao, Y. L., Garrison, S. L., Gonzalez, C., Thweatt, W. D., and Marquez, M.: N-nitrosation of amines by NO₂ and
957 NO: A theoretical study, *J. Phys. Chem. A*, 111, 2200–2205, <https://doi.org/10.1021/jp0677703>, 2007.
- 958 Ziemann, P. J. and Atkinson, R.: Kinetics, products, and mechanisms of secondary organic aerosol formation, *Chem.*
959 *Soc. Rev.*, 41, 6582–6605, <https://doi.org/10.1039/c2cs35122f>, 2012.

960